Roles of inflammatory cells in normal lung development and bronchopulmonary dysplasia

Inauguraldissertationzur Erlangung des Grades eines Doktors der Humanbiologie des Fachbereichs Medizinder Justus-Liebig-Universität Gießen

vorgelegt von Tatiana Kalymbetova
aus Novosibirsk, Russland

Giessen, 2016

Roles of inflammatory cells in normal lung development and bronchopulmonary dysplasia

Aus dem
Max-Planck-Institut für Herz- und Lungenforschung, Bad Nauheim
Prof. Dr Werner Seeger

Betreuer: Prof. Dr. Seeger
Gutachter: Prof. Dr. Kracht

Prüfungsvorsitz: Prof. Dr. Dr. Dettmeyer
Prüfungsmitglied: Prof. Dr. Ziebuhr

Tag der Disputation: 17.02.2016

Table of content

List of figures

List of tables

List of abbreviations

µg	microgram(s)
µl	microliter(s)
µm	micrometer(s)
BPD	bronchopulmonary dysplasia
BSA	bovine serum albumin
CCR2	C-C chemokine receptor type 2
CCL2	C-C motif ligand 2
CSF1	colony stimulation factor 1
CSF1R	colony stimulation factor 1 receptor
CX3CR1	CX3C chemokine receptor 1
CX3CL1	CX3C motif ligand 1
DCs	dendritic cells
ECM	extracellular matrix
EGFP	enhanced green fluorescent protein
ExAM	exudate alveolar macrophages
FACS	fluorescence activated cell sorting
FOV	field of view
$GdCl_3$	gadoliniumchloride
GM-CSF	granulocyte-macrophage colony-stimulating factor
HYX	hyperoxia
h	hour(s)
IP	intraperitoneal
IL	interleukin
KO	knockout
Ly6G	lymphocyte antigen 6 complex, locus G
Ly6C	lymphocyte antigen 6 complex, locus C
LPS	lipopolysaccharide
MAFIA	macrophage Fas-induced apoptosis
M-CSF	macrophage colony stimulation factor
min	minute(s)
ml	milliliter(s)
MLI	mean linear intercept

mm	millimeter(s)
mg	milligram(s)
MCP-1	monocyte chemotactic protein-1
NO	nitric oxide
NOX	normoxia
P	postnatal
PFA	paraformaldehyde
Pop1	population 1
Pop2	population 2
Pop3	population 3
PCR	polymerase chain reaction
$PaCO_2$	partial pressure of carbondioxide in the blood
PaO_2	partial pressure of oxygen in arterial blood
PBS	phosphate buffered saline
qPCR	quantitative PCR
RT	room temperature
ROS	reactive oxygen species
rAM	resident alveolar macrophages
RDS	respiratory distress syndrome
s	second(s)
TH1	T helper 1
TH2	T helper 2
TNF-α	tumor necrosis factor-α
URS	uniform random sampling
WT	wild type

1. Introduction

1.1. Bronchopulmonary dysplasia

The lung is the key organ of respiration in air-breathing animals, with the main function being oxygen transport from the atmosphere into the bloodstream, and carbon dioxide release. This gase exchange takes place in the pulmonary alveoli, which are the respiratory tree terminal ends that outcrop from alveolar ducts, with an average diameter of 200-300 μm. Alveoli consist of an epithelial cells layer supported by extracellular matrix (ECM), and are surrounded by capillaries. Together, these structures form the alveolar-capillary barrier, across which gas exchange takes place. It is clearly advantageous that this barrier should (1) be as narrow as possible to facilitate optimal transit of gas molecules across the barrier, and (2) cover as large a surface area as possible to maximize the area over which gas exchange takes place. Any alveolar architecture disturbances might have serious consequences for gas exchange. In humans, these disturbances can lead to serious diseases such as bronchopulmonary dysplasia (BPD).

Before the 1960s when mechanical ventilation was introduced, premature infants with respiratory distress syndrome either died within the first week of life or survived without respiratory morbidity. The introduction of mechanical ventilation to neonatal intensive care improved infant survival, but resulted in a new form of lung injury. In 1967 Northway (Northway et al. 1967) for the first time described the development of a new chronic lung disease in a group of premature infants who had respiratory distress syndrome (RDS) and received prolonged high oxygen ventilation with high inspiratory pressure, and named this disease “bronchopulmonary dysplasia”. Later the BPD pathophysiology was extensively reviewed (Bancalari et al. 1979, Hislop et al. 1987, Margraf et al. 1991, O'Brodovich and Mellins 1985, Sobonya et al. 1982).

1.1.1. Pathology of bronchopulmonary dysplasia

Bronchopulmonary dysplasia is a chronic lung disease in infants born extremely preterm, occurring typically before 28 weeks of gestation. At this time the human lung is in the saccular stage of development, in contrast with the lung of normal babies born at 36 weeks of gestation, which is in alveolar stage (Fig. 1 A). Some preterm infants are characterized by a prolonged need for supplemental oxygen or positive pressure ventilation which might lead to the development of BPD.

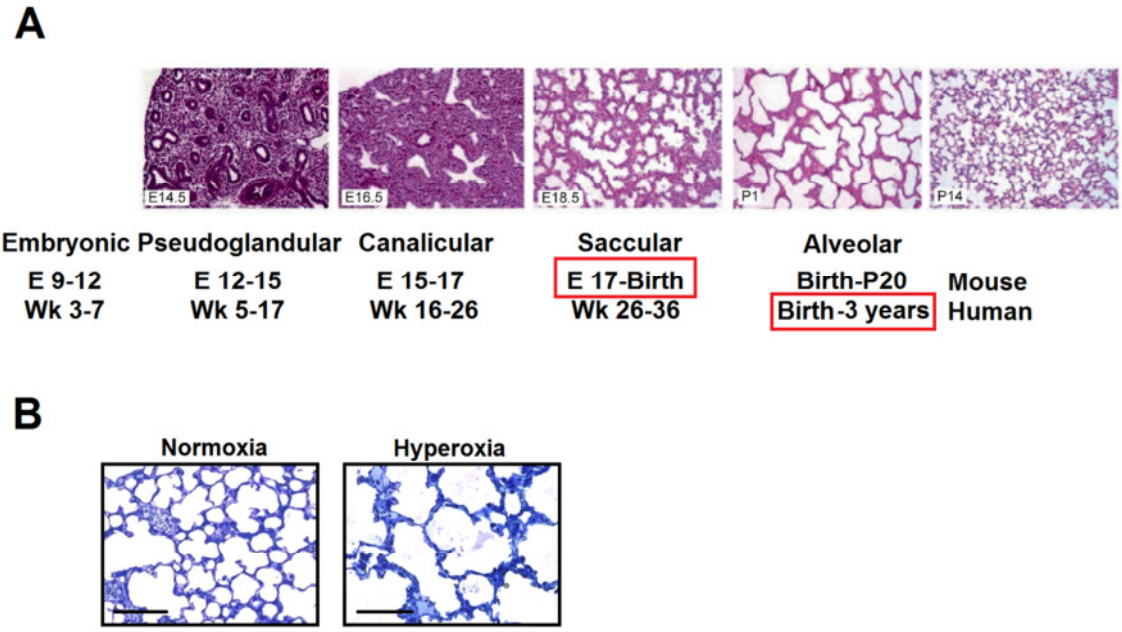

Figure 1 | Mouse model of Bronchopulmonary dysplasia.

A. Stages of human and mouse lung development. Mice are born with lungs in the saccular stage of development that mimics the premature human infants who are born at < 32 weeks of gestation. Modified from (Warburton et al. 2010). **B**. Mouse model of BPD. Within 12 h of birth, wild type (WT) litters were continuously exposed, with their mothers, to either normoxia (21% oxygen) or hyperoxia (85% oxygen) for 10 days. Pups were sacrificed on P10, lungs were plastic-embedded with followed Richardson's staining. Scale bar 100 μm .

Since first description, there have been remarkable changes in the clinical and pathologic phenotype of BPD. This evolution has led researchers and clinicians to use terms "Old BPD" and "New BPD" to differentiate between original form and the currently most commonly seen phenotype. During the first week after birth, the infants with "Old BPD" had typical radiographic findings of respiratory distress syndrome (RDS) with severe worsening towards the latter part of the first week. Thereafter, RDS evolved into a severe chronic obstructive pulmonary disorder with severe airflow limitations and chest radiographs demonstrating multiple cystic areas. Pathologic findings of extensive airway and parenchymal damage in the presence of abnormal lung structure led to the name of the disease, bronchopulmonary dysplasia. Infants that developed BPD and survived often required long periods of assisted ventilation followed by months to years of supplemental oxygen therapy in hospital and then at home.

During the 1970s and 1980s a dramatic improvement in the everyday clinical care of prematurely born infants with acute respiratory disease took place. In addition to many improvements in general intensive care, such as proper nutrition and fluid balance, better understanding of pH, $PaCO_2$ and PaO_2 physiological effects and recognition that pressures usually used during assisted ventilation were causing lung injury, were of critical importance (Gopel et al. 2014, Sun et al. 2015). Since then, several preventive and therapeutic strategies have been developed with variable success (Rojas et al. 2009, Sandri et al. 2004, Soll and Morley 2001, Stevens et al. 2007, Subramaniam et al. 2005, Verder et al. 1999). These include lung protective ventilator strategies, surfactant treatment and nutritional interventions. Together with less hyperoxia and gentler ventilation this led to a virtual disappearance of "old BPD" in infants born at < 32 weeks gestational age (Coalson 2003). Improvements in clinical care also led to a dramatic improvement in the survival rate of very low birth weight infants with < 1,500 g birth weight (Table 1). These extremely premature infants also frequently developed chronic lung disease, however, even though these infants required long term ventilation and supplemental oxygen therapy, the resultant chronic lung disease had a significantly different clinical phenotype from "Old BPD". Often these infants had minimal or mild RDS during the first days of life; chest radiograph usually did not demonstrate cystic areas with interspersed fibrosis and pathologic studies revealed profound differences in lungs histopathology of such infants. The major abnormality was a marked simplification of the distal lung structure with fewer, larger alveoli, reduction in alveolar surface area and thicker septal wall because of a normal lung alveolar septation and pulmonary microvascular development failure (Margraf et al. 1991).

Given the significant clinical, radiologic and pathologic differences between this new type of chronic lung disease in the prematurely born, it is now commonly referred to as "New BPD" (Baraldi and Filippone 2007). In 2000s "New BPD" was characterized by severity in infants < 32 weeks gestational age: mild – supplemental oxygen need for 28 days and room air at 36 weeks corrected gestational age or at discharge; moderate – supplemental oxygen need for 28 days and FiO_2 < 0.3 at 36 weeks corrected gestational age or at discharge; severe – supplemental oxygen need for 28 days and FiO_2 = 0.30 or positive pressure support at 36 weeks corrected gestational age or at discharge (Jobe and Bancalari). It has also been suggested to test infants at 36 weeks gestational age for their need for oxygen (Walsh et al. 2004).

Table 1 Comparisons of clinical variables and frequencies of BPD in surviving ELBW infant populations at two different time periods at the Brindisi Hospital NICU

Variable	ELBW population		*P*-value
	Period 1 July 1, 1986 – June 30, 2002 (N = 72)	Period 2 July 1, 2002 – December 31, 2012 (N = 122)	
Survival rate	72/170 (42.3%)	122/168 (72.6%)	<0.0001
Male/female ratio	24/72 (33.3%)	64/122 (52.4%)	0.0150
Gestational age (wks)	27.2±2.6	27.0±2.0	0.8050
Birth weight (g)	830±121	809±154	0.6986
Rate of inborn births	54/170 (68.3%)	159/168 (94.6%)	<0.0001
Intubation duration (h)	33 (0–120)	144 (121–213)	<0.0001
Total O_2-supplementation (h)	240 (108–504)	400 (216–614)	0.0850
Use of exogenous surfactant	35/72 (48.6%)	109/122 (89.3%)	<0.0001
FiO_2 <0.40 (r)	170 (94–335)	317.5 (169–495)	0.0610
NCPAP (r)	377 (204–558)	600 (504–720)	0.0005
BPD28d	22/72 (30.5%)	48/122 (39.3%)	0.2137
BPD36wk	4/72 (5.5%)	16/122 (13.1%)	0.1452

Values are presented as mean ± SEM. Categorical variables are presented as number of cases with percentages in brackets. ELBW-extremely low birth weight; NCPAP - Nasal continuous positive airway pressure. Modified from (Latini et al. 2013).

Even having all these new approaches for treating and preventing BPD, it remains to be a major cause of mortality in premature infants (Botet et al. 2012, Fanaroff et al. 2003, Horbar et al. 2002, Lemons et al. 2001, Walsh et al.). In addition to mortality, there is considerable morbidity associated with BPD including long-term effects on pulmonary function and neurodevelopment. Babies with BPD have an increased risk for asthma, respiratory-related hospitalizations, and respiratory medication usage after hospital discharge. To prevent postnatal BPD a comprehensive approach is needed (Li Y. et al. 2014b). Thus it is of critical importance to study molecular mechanisms underlying lung growth inhibition and to find key cell types involved in the development and progression of BPD.

1.1.2. Animal models of bronchopulmonary dysplasia

Everything that is known about pathology and pathophysiology of BPD in newborn infants comes from either autopsy material from infants who died with BPD, which means that these samples are received from the most severe cases of BPD; or

from tracheal aspirates from living infants who require mechanical ventilation. That greatly complicates the BPD investigation and makes animal models extremely useful in helping to understand the cause and possible treatment of the disease.

Since the description of BPD in 1967, various animal models were used for studying the disease. One way to induce BPD-like disease in preterm or term animals is prolonged exposure to high oxygen concentrations (usually 85-100% O_2) (D'Angio and Ryan 2014, Li C. et al. 2014a). Hyperoxia-relied animal models of BPD were developed for different animals including neonatal lambs (Hazinski et al. 1985), preterm rabbits (Mascaretti et al. 2009), neonatal rats (Franco-Montoya et al. 2009) and neonatal mice (Tibboel et al. 2013) (Fig. 1 B). All of them demonstrate the BPD-like lung phenotype with characteristic fewer larger alveoli.

Because mechanical ventilation-induced lung injury plays a big role in the pathogenesis of BPD, animal models with mechanically introduced volutrauma were developed. Studies using a chronically ventilated preterm lamb BPD model (Albertine et al. 1999), preterm ventilated baboon model (Coalson et al. 1999, Thomson et al. 2004), high tidal volume ventilated neonatal rats (Wu et al. 2008) as well as invasive ventilated mouse model (Bland et al. , Cannizzaro et al. 2009) demonstrated evidence impaired alveolar formation with an abnormal elastin distribution.

The pre-delivery stimulus to the fetus that induces lung inflammation during preterm labor, sometimes with chorioamnionitis or ruptured membranes, is another risk factor for developing BPD in human infants. (Eriksson et al. 2014, Kramer et al. 2009). To mimic inflammation in animal model, a lipopolysaccharide (LPS) intra-tracheal administration models were developed for number of mammals. Lipopolysaccharide administration increase inflammatory cells and enhanced the inflammatory cytokines expression in preterm lamb model (Polglase et al. 2009), neonate rat model (Franco et al. 2002), as well as mouse models of lung injury (Alvira et al. 2007).

Even though a number of different approaches were developed for studying BPD, there is no perfect model to mimic the human disease. However, these models have many similarities to lung injury in human preterm infants, including disordered lung architecture, alveolar simplification, abnormal pulmonary function, acute inflammatory response with the production of cytokines, chemokines, and growth factors that have been implicated in human disease, development of fibrosis, and abnormal vascular growth factor expression (Berger and Bhandari 2014, Choi et al. 2009, D'Angio and Ryan 2014, O'Reilly and Thebaud 2014).

1.1.3. Inflammation in bronchopulmonary dysplasia

Since the late 1960s, an intensive investigation of BPD pathophysiology took place and soon it became clear that BPD in very premature infants is strongly associated with inflammation. An early study detailing the inflammatory cells influx in ventilated premature infants revealed that patients that develop BPD had influx of both neutrophils and alveolar macrophages to the lung (Ogden et al. 1984). Extensive studies of tracheal aspirates from mechanically ventilated preterm infants that developed BPD showed elevated levels of inflammatory mediators such as interleukin-6 (IL-6) and IL-8 and influx of neutrophils (Bagchi et al. 1994, Groneck et al. 1994, Groneck and Speer 1995, Kotecha et al. 1995, Pierce and Bancalari 1995) (Fig. 2). It is interesting that release of IL-8, a neutrophil chemoattractant, starts as soon as on the third day of oxygen supplementation and mechanical ventilation in preterm infants (Munshi et al. 1997). In later studies of "New BPD" the release of inflammatory mediators and neutrophil influx was also observed (Kim et al. 2004, Papoff et al. 2001). In general, infants that go on to progress to BPD have a persistence of leukocytes in tracheal lavages (Jobe and Ikegami 1998, Ogden et al. 1983).

It also has become evident that a lack of anti-inflammatory mediators in lungs of premature infants may perpetuate the inflammatory response and contribute to the development of BPD (Jones C. A. et al. 1996). Further trials with early administration of anti-inflammatory agent (dexamethasone) to the preterm infants revealed that dexamethasone may slow the progression of BPD (Doyle et al. 2014, Mammel et al. 1983, Rastogi et al. 1996). Thus, influx of inflammatory cells was felt to be related to the pathology of BPD, such as bronchiolar necrosis and loss of appropriate alveolar septation.

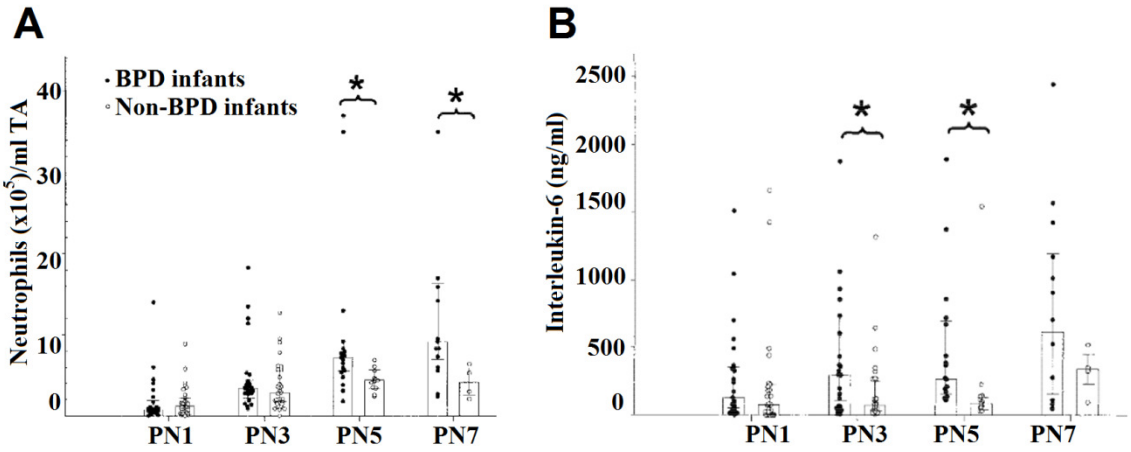

Figure 2 | Levels of neutrophils and inflammatory mediators are up-regulated in preterm infants with BPD.

Tracheal aspirates of preterm infants receiving supplemental oxygen and mechanical ventilation were collected and analyzed for neutrophil number (**A**) using hemocytometer and IL-6 concentration (**B**) using ELISA. Later all infants were divided into two groups: the ones that did not develop BPD (non-BPD infants) and the ones that did (BPD infants). Bronchopulmonary dysplasia was defined as the need for supplemental oxygen at 36 weeks postconceptional age. Median values are represented by bars. Significant up-regulation of neutrophil numbers in BPD infants ($P < 0.05$) was observed on postnatal day 5 (PN5) and IL-6 up-regulation on postnatal day 3. Modified from (Munshi et al. 1997).

Together with understanding that inflammation contributes greatly to the progression of BPD, other risk factors besides the duration of exposure to oxygen and pressure were discovered, such as chorioamnionitis, postnatal infection and the internal host response (Bhandari V. and Gruen 2006, Hayes et al. 2010, Ryan et al. 2008, Speer 2001, 2006, 2009). A number of human studies that attempted to predict BPD from pro-inflammatory factors have been performed (Aghai et al. 2013, Bhandari A. and Bhandari 2009, Bose et al. 2008, Paananen et al. 2009, Schneibel et al. 2013). Ambavalan et al. (Ambalavanan et al. 2009) examined 1067 preterm infants, of which 606 infants developed BPD and found that marked increase in serum levels of IL-8 as early as at 3 days of life and later increases in the level of IL-6 predicted BPD. Another study by Aghai et al. (Aghai et al. 2013) demonstrated correlation between high levels of IFN-γ and interferon-induced protein 10 (IP-10) in tracheal aspirates of mechanically ventilated preterm infant and further BPD development.

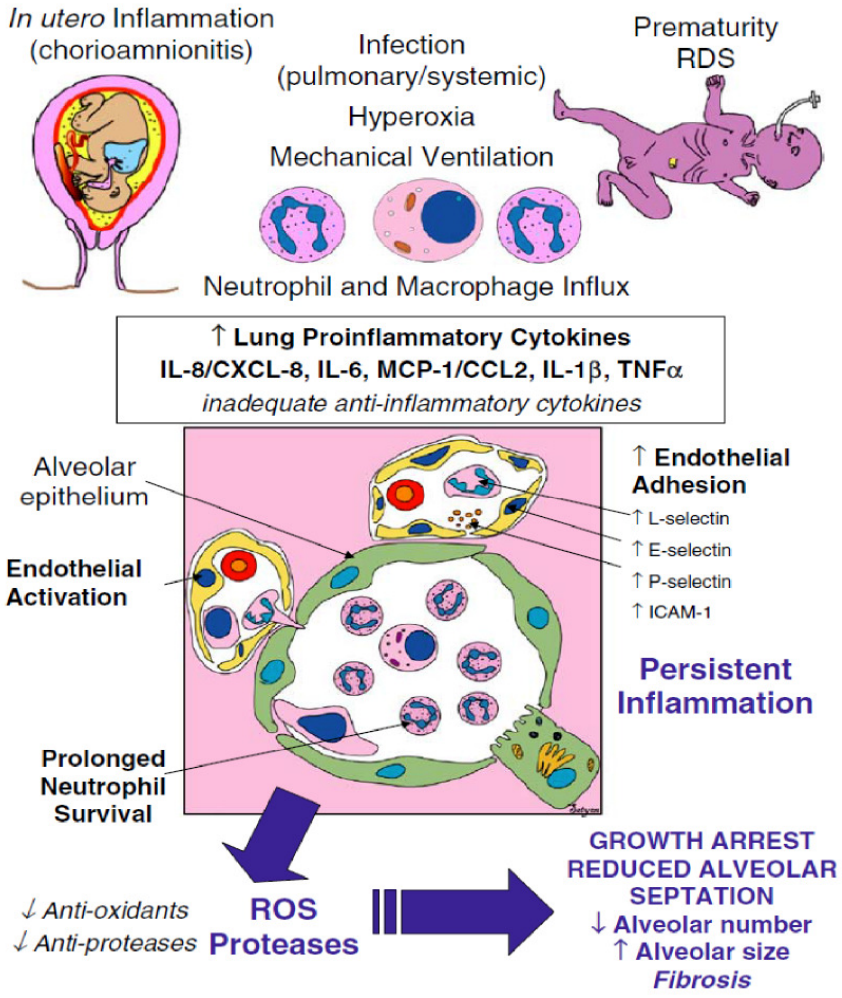

Figure 3 | Inflammation and BPD.

Inflammation plays an important role in the development of BPD. Preterm infants with chorioamnionitis or initial lung injury such as respiratory distress syndrome or with ventilator-induced lung injury, demonstrate an early onset of inflammation with increased levels of pro-inflammatory cytokines and polymorphonuclear cells and macrophages influx. By producing cytokines, proteases and toxic reactive oxygen species (ROS), inflammatory cells can alter the lung's ability to repair, contribute to fibrosis, inhibit secondary septation, alveolarization and normal vascular development and therefore contribute greatly to the progression of BPD (Ryan et al. 2008).

Unfortunately most of the human studies are too small and need to be expanded, but they clearly show that BPD is strongly associated with inflammation and that inflammation can greatly contribute to the development of the disease (Fig. 3).

Intensive studies on inflammation in BPD using various animal models also showed that inflammatory cells and pro-inflammatory mediators play a tremendous role

in BPD. There is a large body of data describing pro-inflammatory mediators up-regulation and leukocytes influx into the lung in response to hyperoxia exposure or to mechanical ventilation using different animal models (Albertine et al. 1999, D'Angio et al. 1999, Sun et al. 2013, Syed and Bhandari 2013, Wagenaar et al. 2004, Wolkoff et al. 2002). For example, there is an increase in both neutrophil and macrophage numbers in neonatal rabbits exposed to 100% oxygen for 9 days (D'Angio et al. 1999). Ten days after hyperoxia exposure, neonatal rats show a massive inflammatory response with a large number of macrophages and neutrophils in air spaces, edema and up-regulation of a number of pro-inflammatory cytokines (Wagenaar et al. 2004) (Fig. 4).

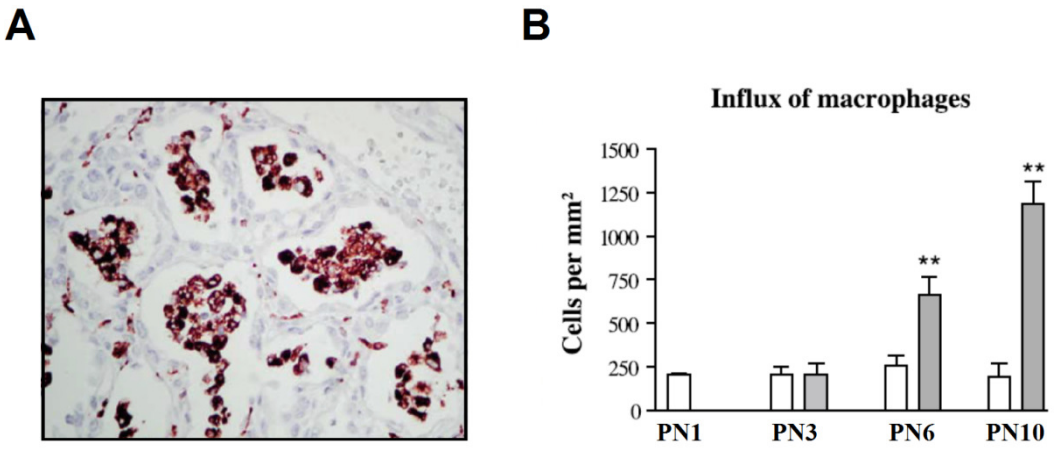

Figure 4 | Macrophages are recruited to the lung in the hyperoxia model of BPD.

A. Macrophage-specific monoclonal antibody (ED1) staining on a formaldehyde-fixed paraffin section of a rat lung on day 10 after oxygen treatment. All pictures were taken at 400× magnification.

B. Quantification of ED1-positive monocytes and macrophages on paraffin sections in oxygen-exposed rat pups (gray bars) and room air–exposed littermates (white bars) as controls. PN – postnatal. Modified from (Wagenaar et al. 2004).

There have now been a large number of animal studies demonstrating that inflammation attenuation improves lung outcome, including specifically improving alveolarization (Anyanwu et al. 2014, Nold et al. 2013, Wagenaar et al. 2014, Wang X. L. and Xue 2009, Weichelt et al. 2013). For example, it was demonstrated that neonatal rats exposed to a combination of caffeine and hyperoxia are less susceptible to lung injury than those exposed to hyperoxia alone and that caffeine blocked the up-regulation of chemokines and pro-inflammatory cytokines and the influx of myeloid leukocytes seen with high oxygen (Weichelt et al. 2013). Another study demonstrated that adding

inhaled nitric oxide (NO) to hyperoxia alters the hyperoxia-induced recruitment of leukocytes into the lung of newborn mice and results in the numbers of alveoli, macrophages and neutrophils approximating those found in room air exposed controls. Addition of inhaled NO to the hyperoxic exposure prevented the hyperoxia-induced up-regulation of ICAM and MCP-1, two factors responsible for leukocyte recruitment (Rose et al. 2010).

Nowadays it is known that inflammation and lung growth arrest observed in BPD are connected; that early inflammatory cytokines up-regulation in tracheal aspirates of preterm infants may be predictive of BPD; that some anti-inflammatory therapies using corticosteroids proved to be beneficial. But, with the knowledge acquired in the past 50 years, unfortunately there is still no existing therapy for BPD, which makes it of critical importance to continue investigations on inflammation and lung alveolarization arrest associated with BPD (Bhandari V. 2014).

1.2. Inflammation

Inflammation is a protective immune response that involves molecular mediators, blood vessels and immune cells such as neutrophils and macrophages. Inflammation purpose is to eliminate the initial cause of cell injury, clear out necrotic cells and debris, and to initiate tissue repair. Too little inflammation could lead to progressive tissue destruction by the harmful stimulus and, in contrast, chronic inflammation may lead to development of diseases, such as hay fever, periodontitis, atherosclerosis, and even cancer. Therefore, inflammation has to be tightly regulated.

1.2.1. Neutrophils

Neutrophils are the most abundant type of white blood cells in mammals formed from stem cells in the bone marrow and represent an essential part of the innate immune system. Neutrophils are phagocytic granulocytes, short-lived and highly motile. Lymphocyte antigen 6 complex, locus G (Ly6G) together with Ly6C is a component of the myeloid differentiation antigen Gr-1 that predominantly present on neutrophils, making it a good lineage marker.

During the acute phase of inflammation, for example as a result of bacterial infection or environmental exposure, neutrophils are one of the first-responders of inflammatory cells to migrate towards the site of inflammation. Following chemical signals such as IL-8, neutrophils migrate through the blood vessels and then through

interstitial tissue to the site of injury. Neutrophils are massively recruited to the lung in response to hyperoxia in preterm and term animal models of BPD and a study using targeted neutrophil depletion in neonate rat BPD model suggest the role of this cell in inflammatory lung injury (Auten et al. 2001).

Several investigators have shown that neutrophils of neonatal mice appear to have decreased apoptosis and prolonged survival compared to neutrophils of adult mice, and this may also increase the neutrophil contribution to the inflammatory process and lung injury in preterm infants. Specific factors involved are decreased expression of pro-apoptotic proteins Bax, Bad and Bak, and Fas receptor and decreased activity of caspase 3 in neonatal neutrophils compared with adult neutrophils (Hanna et al. 2005). Kotecha et al. (Kotecha et al. 2003) performed pulmonary lavage on 32 babies with RDS who later fully recovered (RDS group), with RDS who later developed BPD (BPD group), and control infants without RDS who did not receive high oxygen ventilation. They found that neutrophil apoptotic activity in lavage samples on day 1 of age was much lower in BPD group than in control group, and there was a significant correlation between higher apoptotic activity and increasing gestational age which shows that inappropriate suppression of neutrophil apoptosis and their longer survival may be associated with a poor outcome in newborn infants with respiratory failure.

1.2.2. Macrophages

Macrophages are professional phagocytic cells, often long lived, that are present in all organs to maintain tissue integrity, clear debris and respond rapidly to initiate repair after injury or innate immunity after infection (Hume 2008). Macrophages develop from hematopoietic stem cells originating in both fetal and bone marrow hematopoiesis. During the development, coincident with the postnatal bone formation, fetal liver haematopoiesis declines and is completely replaced by bone marrow haematopoiesis. This definitive haematopoiesis is the source of circulating monocytes and from which it has been considered that all resident macrophages in tissues are derived. Contrary to this idea some fate-mapping models suggest that several types of tissue macrophages such as Kupffer cells, epidermal Langerhans cells, and microglia arise from primitive hematopoietic progenitors present in the yolk sac of the fetus independently of the monocyte lineage (Ginhoux et al. 2010, Schulz et al. 2012). It was also suggested that maintenance and local expansion of microglia are solely dependent on the self-renewal of central nervous system resident macrophages in

neurodegenerative disease (Ajami et al. 2007). Another study demonstrated that local macrophage proliferation, rather than recruitment from the blood, occurred during T helper 2 (TH2)-related pathologies (Jenkins et al. 2011). These data suggest that circulating monocytes do not give rise to all resident macrophages in the organism and that different populations of tissue macrophages can have different precursors.

To be differentiated into macrophages or other related cell types, hematopoietic stem cells require a secreted cytokine colony stimulating factor 1 (CSF1 or M-CSF). Colony stimulating factor 1 is produced constitutively by a wide variety of mesenchymal and epithelial cells and acts on target cells by binding to CSF1R, a member of the type III protein tyrosine kinase receptor family. Although most bone marrow-derived populations depend primarily on CSF1 signaling via CSF1R for their development and survival, some self-renewing tissue macrophages like microglia, require tissue-restricted signals derived from IL-34, the alternate ligand of CSF1R (Wang Y. et al. 2012). Hematopoietic stem cells differentiate into monoblasts, bipotent cells that are monocyte precursors in the bone marrow. After monoblasts differentiate into monocytes, they circulate in the bloodstream for about one to three days and then move into tissues to either replenish resident macrophages under normal states or to move quickly to sites of infection in response to inflammation signals and differentiate into macrophages and dendritic cells to elicit an immune response. There are two major monocyte subsets expressing different chemokine receptor patterns: $CCR2^{+}$; $CX3CR1^{lo}$; $Ly6C^{hi}$ and $CCR2^{-}$; $CX3CR1^{hi}$; $Ly6C^{lo}$ monocytes. Chemokine signaling in the tissues leads to recruitment of all subsets of monocytes and is primarily mediated by the chemokine receptors CCR2 and CX3CR1, and their ligands CCL2 (monocyte chemotactic protein-1, MCP-1) and CX3CL1 (fractalkine), respectively (Ancuta et al. 2003, Shantsila et al. 2011). The monocyte subset that is recruited to tissues in response to inflammation and differentiates into inflammatory exudate macrophages is known to be the $CCR2^{+}$; $CX3CR1^{lo}$; $Ly6C^{hi}$ subset.

Among tissue resident macrophages, alveolar macrophages have a unique phenotype. Unlike resident macrophages of other tissues, they are highly autofluorescent, express high integrin CD11c levels and low phagocytic receptor CD11b levels, and high lectin SiglecF levels, that makes alveolar resident macrophages to be easily recognized among other myeloid cells of the lung and other organs (Gautier et al. 2012, Misharin et al. 2013). Resident alveolar macrophages (rAM) start accumulating in the lung only after the mouse is born and rAM number is increasing

during alveolarization. Resident alveolar macrophages are derived from fetal monocytes that differentiate into long-lived cells in the first week of life via GM-CSF (Guilliams et al. 2013).

The role of macrophages in disease development is of particular interest because macrophages can exhibit distinctly different functional phenotypes, broadly characterized as classically activated pro-inflammatory (M1) and alternatively activated tissue-reparative anti-inflammatory (M2) phenotypes. M1 and M2 polarization of macrophages have largely been defined through *in vitro* stimulation experiments (Stein et al. 1992). Derivation of macrophages from bone marrow in the presence of M-CSF and TH1-type cytokine IFN-γ treatment results in M1-polarized macrophages; and in the presence of GM-CSF and TH2-type cytokines IL-4 and IL-13 treatment results in M2-polarized macrophages. M1-polarized macrophages demonstrate increased secretion of pro-inflammatory cytokines such as IL-6, IL-8 and TNF-α, increased expression of activation receptors such as CD40 and CD80,high production of reactive nitrogen and oxygen intermediates, promotion of TH1 response, and express tumor-suppressive activities and strong microbicidal activities. Macrophage polarization towards classically activated M1 phenotype is associated with NF-κB and STAT1 pathway activity (Gordon and Taylor 2005). Macrophage switch toward alternatively activated M2-macrophages that produce IL-10 and TGF-β and express mannose receptor CD206, induce resolution of inflammation and tissue regeneration (Gordon 2003). Distinctly different roles for these macrophages subtypes have been reported in injury and recovery in different organs (Arnold et al. 2007, Duffield et al. 2005, Nahrendorf et al. 2007) and it was demonstrated that M1 macrophages can themselves convert into anti-inflammatory macrophages with an M2 wound-healing phenotype (Arnold et al. 2007, Biswas and Mantovani 2010). During alveolarization rAM polarize to a M2 anti-inflammatory phenotype, localize to sites of branching morphogenesis and increase in number during the alveolarization stage of normal lung development(Jones C. V. et al. 2013). A study done by Rozycki et al. (Rozycki et al. 2002) demonstrated that when alveolar macrophages obtained from preterm and term rabbits were incubated in 95% oxygen overnight, only “preterm” macrophages showed a significant increase in IL-1β and IL-8 mRNA expression and an intracellular oxygen radical content, depicting that “preterm” alveolar macrophages switch phenotype from M2 to M1 pro-inflammatory phenotype under hyperoxia conditions. Such enhanced inflammatory

cytokine response to oxygen may be one mechanism involved in the early development of chronic lung disease in premature infants.

Another study done by Jankov et al. (Jankov et al. 2003) demonstrated that abrogated macrophage influx in newborn rat hyperoxia model by means of intraperitoneal gadoliniumchloride ($GdCl_3$) completely abrogates hyperoxia-induced increased macrophage numbers and increased ROS, suggesting that increased macrophage numbers in the lungs of newborn hyperoxia-exposed rats strongly contributes to ROS-mediated injury.

All these findings suggest a possible role of macrophages in the development of chronic lung diseases of premature infants and, in particular, BPD. Therefore, the inflammation impact on lung organogenic populations of macrophages should be considered when investigating the neonatal lung damage and dysregulation, associated with preterm birth.

2. Hypothesis and aims of study

Bronchopulamonary dysplasia is a severe disease of extremely preterm infants that remains a main major cause of mortality in premature infants (Fanaroff et al. 2003, Horbar et al. 2002, Lemons et al. 2001, Walsh et al.). In addition to mortality, there is considerable morbidity associated with BPD including long-term effects on pulmonary function and neurodevelopment. Several preventive and therapeutic therapies were introduced in the last years, including preventive ventilation and better nutrition, early surfactant administration and corticosteroid treatment (Doyle et al. 2014, Rojas et al. 2009, Sandri et al. 2004, Soll and Morley 2001, Stevens et al. 2007, Subramaniam et al. 2005, Verder et al. 1999). However, even though the pathology of BPD became milder since its first description in 1967 and introduction of surfactant and dexamethasone therapies, there is still no potential treatment for BPD.

There is a growing body of evidence that BPD is strongly associated with inflammation. Massive inflammatory cells influx together with inflammatory cytokines release is observed in patients that developed BPD (Kim et al. 2004). A number of human studies attempted to predict BPD from pro-inflammatory factors have been performed (Aghai et al. 2013, Bhandari A. and Bhandari 2009, Bose et al. 2008, Paananen et al. 2009, Schneibel et al. 2013). Therefore it was hypothesized that inflammatory cells, in particular neutrophils and macrophages, might play an important role in the development of BPD and might contribute to BPD progression.

The aim of this study was:

To deplete different types of inflammatory cells and study macrophage- and neutrophil-specific roles in the arrested lung development associated with BPD. To deplete different types of macrophages, CCR2 knockout (CCR2 KO) and Macrophage Fas-Induced Apoptosis (MAFIA) transgenic mice were used. To specifically deplete neutrophils, anti-Ly6G monoclonal antibody was used.

3. Material and methods

3.1. Materials

3.1.1. Technical equipment

Autoclave; Systec, Germany

BD LSRII flow cytometers with DIVA software, BD Biosciences, USA

BD FACSAriaIII with DIVA Software, BD Biosciences, USA

Cell culture sterile working bench; Thermo Scientific, USA

Cell strainers: 100, 40 μm; BD Falcon™, USA

Countess® cell counter; Invitrogen, UK

Cytospin™ 4 Cytocentrifuge, Thermo Scientific, USA

Espresso personal microcentrifuge; VWR, USA

InoLab® pH meter; WTW, Germany

Isoplate™ B&W 96-well plate; PerkinElmer, USA

Leica microscope DM4000B, Leica, Germany

MicroAmp® FAST 96-well reaction plate; Applied Biosystems, USA

Microcentrifuge tubes: 0.5, 1.5, 2 ml; Eppendorf, Germany

Minispin® centrifuge; Eppendorf, Germany

Multifuge 3 S-R centrifuge; Heraeus, Germany

NanoZoomer XR C12000 Digital slide scanner, Hamamatsu, Japan

NanoDrop® ND 1000; PeqLab, Germany

Pipetboy; Eppendorf, Germany

Pipetmans: P10, P20, P100, P200, P1000; Gilson, France

Pipetman filter tips: 10, 20, 100, 200 and 1000 μl; Greiner Bio-One, Germany

Refrigerated microcentrifuge CT15RE; VWR, USA

Serological pipettes: 2, 5, 10, 25, 50 ml; Falcon, USA

StepOnePlus™ Real-Time PCR system; Applied Biosystems, USA

Test tubes: 15, 50 ml; Greiner Bio-One, Germany

Vasofix® Safety intravenous catheter; B. Braun, Germany

Vortex mixer; VWR, USA

MicrotomeLEICA SM 2500, Leica, Germany

3.1.2. Chemical and reagents

2-Propanol; Merck, Germany

Agarose; Promega, Germany

Anti-Ly6G and Ly6C monoclonal antibody; BD Pharmingen, USA

Anti-CD45; BioLegend, USA

Anti-Gr-1; BioLegend, USA

Anti-CD11c; BioLegend, USA

Anti-CD11b; BioLegend, USA

Anti-SiglecF; BD Pharmingen, USA

Anti-MHCII; eBioscience, USA

Anti-CD40; BioLegend, USA

Anti-CD206; BioLegend, USA

Bovine serum albumin; Sigma-Aldrich, Germany

Bromophenol blue; Sigma-Aldrich, Germany

Cacodylate; Sigma-Aldrich, Germany

Calcium chloride; Sigma-Aldrich, Germany

Dispase; BD Biosciences, USA

DMSO; Sigma-Aldrich, Germany

DNase I; Serva, Germany

dNTP mix; Promega, USA

Dulbecco's modified Eagle's medium; Gibco BRL, Germany

Dulbecco's phosphate buffered saline, 10×; PAA Laboratories, Austria

Dulbecco's phosphate buffered saline, 1×; PAA Laboratories, Austria

EDTA; Sigma-Aldrich, Germany

Eosin; Sigma-Aldrich, Germany

Ethanol 70%; SAV-LP, Germany

Ethanol 99%; J.T. Baker Mallinckrodt Baker B.V., Netherlands

Ethanol absolute; Riedel-de Hëan, Germany

Ethidium bromide; Promega, USA

FACS buffer, eBioscience, USA

Formaldehyde, 37%; Sigma-Aldrich, Germany

Formamide; Fluka, Germany

Giemsa's azur eosin methylene blue solution; Merck, Germany

Glutaraldehyde; Sigma-Aldrich, Germany

Glycol methacrylate (Technovit7100), Heareus Kulzer

HEPES; PAA Laboratories, Austria

Hydrochloric acid; Sigma-Aldrich, Germany

Isoflurane; CP-Pharma, Germany

Magnesium chloride; Sigma-Aldrich, Germany

Magnesium chloride, 25 mM; Applied Biosystems, USA

May-Grünwald's eosin-methylene blue solution; Merck, Germany

Methanol; Fluka, Germany

MuLV reverse transcriptase; Applied Biosystems, USA

Normal rabbit IgG; Santa Cruz Biotechnology, USA

Nuclease-free water; Ambion, USA

Osmium tetroxide; Sigma-Aldrich, Germany

Paraformaldehyde; Sigma-Aldrich, Germany

PCR buffer II, 10×; Applied Biosystems, USA

Platinum® SYBR® Green qPCR SuperMix UDG kit; Invitrogen, USA

Proteinase K; Promega, USA

RNeasy Mini Kit; Qiagen, Netherlands

Random hexamers; Applied Biosystems, USA

RNase inhibitor; Applied Biosystems, USA

Sandoglobulin; Novartis, Switzerland

Select agar; Sigma-Aldrich, Germany

Sodium azide; Sigma-Aldrich, Germany

Sodium chloride; Merck, Germany

Trypan blue; Fluka, Germany

Uranyl acetate; Sigma-Aldrich, Germany

3.2. Methods

3.2.1. Animal experiments

All animal experiments were approved by local authorities, the Regierungspräsidium Darmstadt (approval B2/358).

3.2.1.1. CCR2 KO mice

C-C chemokine receptor type 2knockout mice (B6.129S4-Ccr2tm1Ifc/J) have a C57/Bl6/J background and were obtained from the Jackson Laboratory (Boring et al. 1997). Double KO mice are viable, fertile, normal in size and do not display any physical or behavioral abnormalities. It has been demonstrated that CCR2 KO mice have impaired monocyte migration and reduced TH1 cytokine responses (Boring et al. 1997).

3.2.1.2. Macrophage Fas-Induced Apoptosis (MAFIA) transgenic mice

Macrophage Fas-Induced Apoptosis (MAFIA) (C57BL/6-Tg(Csf1r-EGFP-NGFR/FKBP1A/TNFRSF6)2Bck/J) mice have a mixed background between C57/Bl6/J and C57/Bl6/N mice and were obtained from the Jackson Laboratory. An FKBP-Fas suicide construct (containing an IRES sequence, human low affinity nerve growth factor receptor, two copies of the 12kDa human FK506 binding protein 1A (FKBP12), and the intracellular domain region of the Fas gene) was inserted immediately downstream of the Enhanced Green Fluorescent Protein (EGFP, Clonetech) gene. This entire construct was placed under the control of the mouse colony stimulating factor 1 receptor (CSF1R) promoter. The mutant human FKBP12 preferentially binds the dimerization drug AP20187, thus resulting in apoptosis of CSF1R-positive cells. Homozygous mutant mice are viable, fertile, normal in size and do not display any physical or behavioral abnormalities. MAFIA mice are well described in the literature and dosage of AP20187 ligand is well established for adult mice (Burnett et al. 2004). In our studies we used same dosage for neonate pups. Three introperitoneal (IP) injections of AP20187 ligand (10 mg / kg body weight) in 20 µl vehicle (4% ethanol, 10% PEG 400, 2% Tween 20) volume were performed on postnatal day 1 (P1), P2 and P3 and one additional on P7 in treated groups; control vehicle injections were performed in control groups.

3.2.1.3. Neutrophil depletion in neonate WT mice

Neutrophils were depleted using neutrophil-specific anti-Ly6G and Ly6C monoclonal antibody (clone RB6-8C5, BD Pharmingen). Such method is well described in the literature and dosage is established for adult mice (Daley et al. 2008, Dhaliwal et al. 2012). In our study the same dosage for neonate mice was used. C57/Bl6/J pups received intraperitoneal injections of antibody (1 mg / kg body weight) in 20 µl of sterile saline on every second day (on P1, P3, P5, P7 and P9) as depletion is very rapid and it lasts for 48 h. Control pups receive vehicle injections on same days.

3.2.1.4. Mouse model of bronchopulmonary dysplasia

Alveolarization arrest was induced by exposing pups to normobaric hyperoxia (85% O_2) as previously described. This model is well described and characterized (Berger and Bhandari 2014). Within 12 h of birth, litters were randomized and continuously exposed, with their mothers, to either normoxia (21% O_2) or hyperoxia (85% O_2) for 10 days. Nursing dams were rotated between normoxia and hyperoxia every day to minimize oxygen toxicity. Dams and pups received food ab libitum and were kept on 12 h light-dark day-cycle. Pups were sacrificed on P10 with an isofluoran overdose followed by thoracotomy and lung extraction.

3.2.2. Design-based stereology

3.2.2.1. Lung fixation and embedding

Lungs were fixed by intratracheal instillation of 1.5% paraformaldehyde, 1.5% glutaraldehyde in 150 mM HEPES, pH 7.4 at hydrostatic pressure of 20 cmH_2O at 4 °C. Tissue blocks were collected according to systematic uniform random (URS) sampling and total volume of the lung ($V_{(lung)}$) was measured by Cavalieri's principle using Stepanizer software. Lungs were embedded in agar and cut into 2 mm slices, treated with sodium cacodylate, osmium tetroxide, uranyl acetate and embedded in glycol methacrylate. Sections of 2 µm were cut and each 1st and 3rd continuous sections were stained with Richardson's stain. Slides were scanned with NanoZoomer slide scanner and lung structure parameters counts were performed using Visiopharm NewCast computer-assisted stereology system (VIS 4.5.3). Structural analysis included determination of mean linear intercept (l_m), alveolar septal wall thickness (τ(sep)) and alveolar number ($N_{(alv/par)}$).

3.2.2.2. Stereological measurements

First, all lung pieces on the slide were masked and fields of views (FOV) were defined (Fig. 5 A, B). Using a dot grid each FOV was first analyzed for parenchyma/non-parenchyma by counting numbers of points that hit parenchyma or non-parenchyma, and a final volume of the lung parenchyma was calculated using formula

$V_{(par/lung)}[cm^3] = V_{(lung)}[cm^3] \times Vv_{(par/lung)}[\%]$, where Vv is volume density.

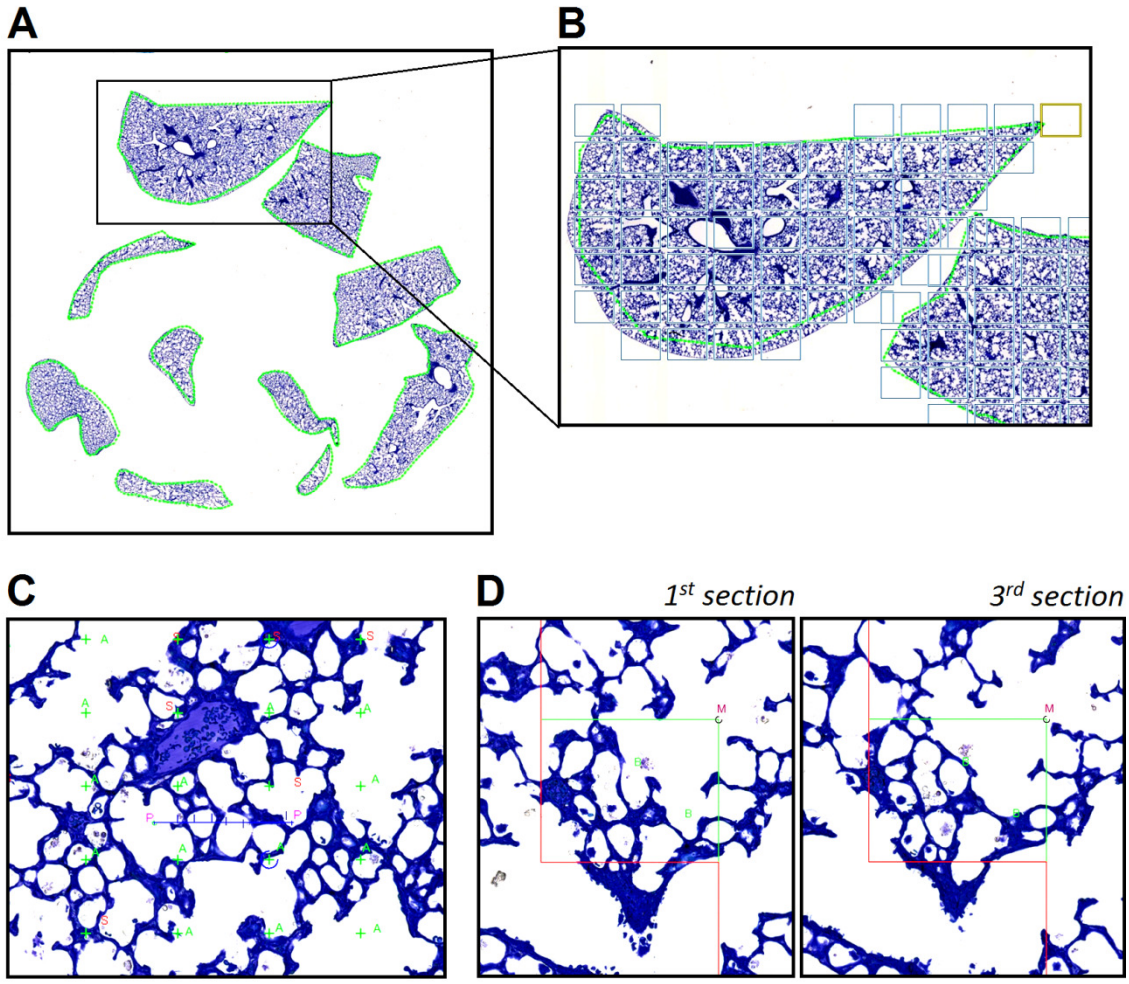

Figure 5 | Stereological analysis of lung structure.

2 µm sections of plastic embedded mouse lungs stained with Richardson's stain and scanned with NanoZoomer slide scanner, were analyzed with Visiopharm NewCast computer-assisted stereology system. First all lung sections were masked (**A**) and fields of views were defined (**B**). For counting septal wall thickness and MLI a dot grid and an intersection line were used for each FOV (**C**) and number of dots that hit septa (S) and alveolar space (A) as well as intersections (I) and parenchyma (P) were counted. **D.** To count alveolar number a physical dissector was used. 1st and 3rd continuous sections were used and a number of bridges (B) were counted using counting frame (M).

After that each FOV was analyzed for alveolar and septal volumes by counting dots that fall on either alveolar and duct space (A) or septa (S) (Fig. 5 C). To count intersect density (I_L), the intersection counting was performed and number of intersections (I) and parenchyma points (P) were counted for each intersection line for each FOV (Fig. 5 C). The intersection density was calculated using the formula $I_L = I / (l(p) \times P)$, where l(p) is length per point [μm]. The surface density $S_v = 2I_L$ and finally surface density of parenchyma $S_{(sept/par)} = S_v \times V_{(par/lung)}$. Knowing this parameter, septal wall thickness can be estimated: $\tau(sep)[\mu m] = 2V_{(sept/par)} / S_{(sept/par)}$. Mean linear intercept (l_m) can also be calculated using the formula $l_m = 4V_{(alv/lung)} / S_{(sept/par)}$.

Alveolar number was estimated using a physical dissector with 4 μm hight (h) (Fig. 5 D). Three continuous 2 μm sections of the lung were cut and 1st and 3rd sections were used for the physical dissector. On each two matching FOV a counting frame was put and numbers of bridges (B) and frames (M) were counted. Number of alveoli was calculated using the following formula:

$$N_{(alv/par)} = B \times V_{(par/lung)}[cm^3] / (2M \times h[cm] \times A[cm^2]),$$

where A is the counting frame surface. For each parameter coefficient of error (CE), coefficient of variation (CV) and ratio between squared (CE^2/CV^2) were measured to be < 0.5 to ensure the precision of the measurements.

3.2.3. Flow cytometry analysis and sorting

Multiparameter flow cytometry was performed using LSRII flow cytometer equipped with DIVA software. Cell sorting was performed using a FACSAriaIII equipped DIVA Software. Gates were set according to unstained controls and isotype controls for CD40 and CD206 antibodies.

3.2.3.1. Whole lung single cell suspension preparation

Lungs of 10 days old pups were instilled with 37 °C Dispase through trachea, isolated and incubated in 37 °C Dispase for 30 minutes. Then, they were cut into fine pieces in 5 ml DMEM media with 2.5% HEPES and 0.01% DNAse I and single-cell suspensions were obtained by passing lung homogenates through 24G syringes before being passed through 100 and 40 μm cell strainers and centrifuged 1400 rpm for 10 min at 4 °C. Supernatant was trashed and cell pellets were resuspended in 5 ml FACS buffer

(PBS, 1% BSA, 0.05% NaN_3). Viable cell count was determined using Trypan Blue stain.

3.2.3.2. Peripheral blood single cell suspension preparation

Mouse pups were anesthetized with isoflurane; 1 ml syringes and 30G needles were prepared for blood collection by flushing with 4% citrate-solution and 300 µl of total blood was drawn by cardiac puncture and collected in tubes with 1/10 of citrate solution and kept on ice. Samples were centrifuged for 20 min at 4 °C. Plasma was removed and the remaining blood cells were washed with FACS buffer (PBS, 1% BSA, 0.05% NaN_3) and fixed with 0.1% PFA.

3.2.3.3. Staining for FACS analysis and sorting

For staining cells were incubated with blocking reagent and antibodies against CD45, Gr-1, CD11c, CD11b, SiglecF, MHCII and CD40 and CD206 or their isotype controls in the dark for 15 min at 4 °C and were then washed with FACS buffer.

3.2.4. Gene expression analysis

3.2.4.1. mRNA isolation from sorted cell populations

At least 100 000 cells were FACS sorted for each experimental group, total RNA from cells was isolated using a QiagenRNeasy Mini Kit according to the manufacturer's instructions. The quantification and purity of isolated RNA was determined with a NanoDrop® ND 1000 and cDNA synthesize was performed from RNA preparations with A260/280 absorbance ratio above 1.90.

3.2.4.2. cDNA synthesis

Reverse transcription was performed on total RNA using MuLV reverse transcriptase and random hexamer oligodeoxyribonucleotides. To perform cDNA synthesis, 20 µl of RNA was denatured at 70 °C for 10 min, transferred onto ice, and supplemented with 20 µl of reverse transcription mixture. The mixture was incubated at 21 °C for 10 min, followed by an RNA synthesis step at 43 °C for 1 h 15 min. The final incubation at 99 °C for 5 min was performed to inactivate MuLV reverse transcriptase.

Reverse transcription mixture	
10×PCR buffer II	4 µl
25 mM $MgCl_2$	8 µl
H_2O	1 µl
Random hexamers	2 µl
RNase inhibitor	1 µl
10 nM dNTP mix	2 µl
MuLV reverse transcriptase	2 µl
Total volume	**20 µl**

3.2.4.3. Real time quantitative PCR

Analysis of the gene expression at the mRNA level was performed by real-time quantitative polymerase chain reaction (rtPCR) using a Platinum® SYBR® Green rtPCR SuperMix UDG kit and a StepOnePlus™ Real-Time PCR System. Primers used in the gene expression analyses are listed in Table 2.

Gene	Species	Forward and reverse primers sequences (5'-3')
PolR2A	mouse	CTAAGGGGCAGCCAAAGAAAC CGGATCTCAACATACGACTTACC
HSPA8	mouse	TCTCGGCACCACCTACTCC CTACGCCCGATCAGACGTTT
CD68	mouse	TTCTCCCACCACAAATGGCA CTTGGACCTTGGACTAGGCG

Conditions of the thermal cycling reaction were as follows: 50 °C for 2 min, 95 °C for 5 min, 40 cycles of 95 °C for 5 s, 59 °C for 5 s, 72 °C for 30 s. The samples were subjected to melting curve analysis to exclude the possibility of primer-dimer formation. A constitutively expressed mouse PolR2A reference gene was used as a

reference gene for rtPCR reactions. Target gene expression was assessed with the comparative Ct method (ΔCt method) and calculated with the equation:

ΔCt = Ct (reference) – Ct (target).

3.2.5. Cytospin

Cells obtained by sorting were transferred on the microscopic slides using Thermo Scientific™ Cytospin™ 4 Cytocentrifuge followed by hematoxylin and eosin staining. Pictures were taken with Leica microscope DM4000B.

3.2.6. Statistical analysis

Values are presented as mean ± SEM. Statistical comparisons between means of two groups were performed using unpaired Student's t-tests. For multiple comparisons, statistical analysis was performed using one-way ANOVA followed by a Tukey's post-hoc test. *P* values less than 0.05 were considered significant.

4. Results

4.1. Inflammation in the neonate hyperoxia mouse model of BPD

Neonate wild type (WT) mouse pups from the first day of life (P1) were exposed, with their mothers, to either 21% oxygen (normoxia group) or 85% oxygen (hyperoxia group) for 10 days (until P10) and inflammation was assessed by flow cytometry analysis. As expected, neutrophils ($CD45^+$; $Gr\text{-}1^+$) were massively recruited to the lung under hyperoxic conditionsre; the population of rAM ($CD11c^+$; $SiglecF^+$; $CD11b^-$) was found to be eliminated in hyperoxia group and ExAM ($CD11c^+$; $CD11b^+$; $MHCII^{interm}$) were recruited to the lung in response to hyperoxia exposure (Fig. 6).

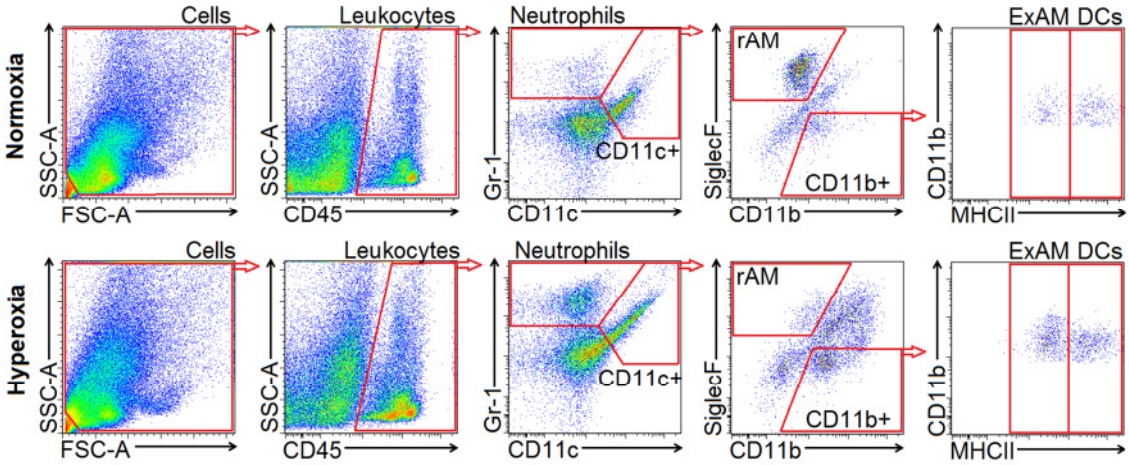

Figure 6 | Neutrophils and ExAM are recruited and rAM are eliminated in mouse pups exposed to hyperoxia.

Whole lung homogenates of P10 WT mouse pups exposed to normoxia versus hyperoxia (5 pups in each group) were assessed for inflammatory cell populations using flow cytometry. Neutrophils were defined as $CD45^+$; $Gr\text{-}1^+$ cells; rAM as $CD11c^+$; $SiglecF^+$; $CD11b^-$; ExAM as $CD11c^+$; $CD11b^+$; $MHCII^{interm}$; dendritic cells (DCs) as $CD11c^+$; $CD11b^+$; $MHCII^{hi}$. Representative flow cytometry plots are illustrated.

These results demonstrate that there is a massive inflammation in response to hyperoxia exposure and raze a possibility that inflammatory cells such as neutrophils and ExAM can contribute to the arrested lung development associated with BPD.

4.2. CCR2 KO mice reveal abrogated ExAM recruitment to the lung in response to hyperoxia compared with WT controls

To assess the role of ExAM in the arrested lung development, CCR2 KO mice were exposed to hyperoxia for 10 days. First, the inflammatory response was examined by flow cytometry analysis that revealed, as expected, a pronounced abrogation of ExAM recruitment to the lung in response to hyperoxia exposure compared with WT control pups exposed to hyperoxia (Fig. 7, 9). Neutrophils were recruited to the lung to the same extent as it was observed in WT controls and rAM population was eliminated in the hyperoxia exposed group (Fig. 7, 9).

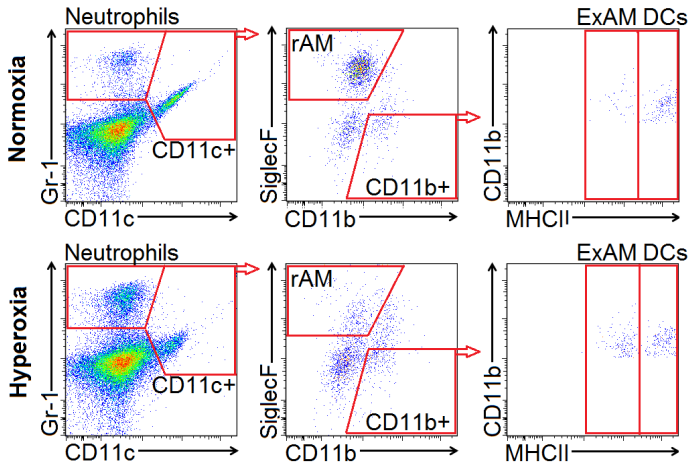

Figure 7 | ExAM recruitment to the lung is abrogated in CCR2 KO pups exposed to hyperoxia. Whole-lung homogenates of P10 CCR2 KO mouse pups exposed to normoxia versus hyperoxia (4 pups per group) were assessed for inflammatory cell populations using flow cytometry analysis. Neutrophils were defined as $CD45^{+}$; $Gr\text{-}1^{+}$ cells; rAM as $CD11c^{+}$; $SiglecF^{+}$; $CD11b^{-}$; ExAM as $CD11c^{+}$; $CD11b^{+}$; $MHCII^{interm}$; dendritic cells (DCs) as $CD11c^{+}$; $CD11b^{+}$; $MHCII^{hi}$. Representative flow cytometry plots are illustrated.

4.3. MAFIA mice demonstrate rAM depletion and no neutrophil recruitment in response to hyperoxia with clear ExAM populations both in normoxia and hyperoxia exposed groups

To assess the role of CSF1R-expressing cells in the arrested lung development associated with BPD, MAFIA transgenic mice were used. Neonate MAFIA pups received four intraperitoneal (IP) injections of AP20187 ligand on P1, P2, P3 and P7 to deplete all CSF1R-expressing cells and were exposed from P1 to normoxia versus

hyperoxia until P10. Depletion efficiency was controlled with flow cytometry analysis by checking GFP reporter (Fig. 8 A) and appeared to be more than 85%.

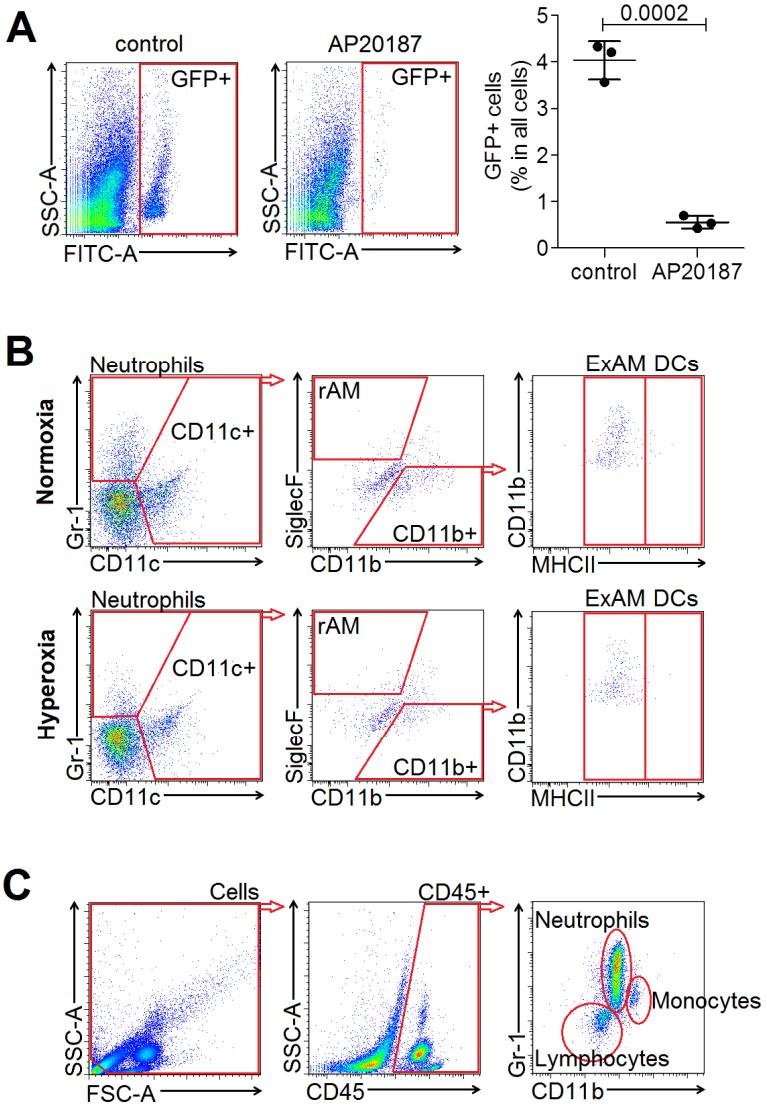

Figure 8 | MAFIA mice demonstrate rAM depletion and no neutrophil recruitment in response to hyperoxia with clear ExAM populations both in normoxia- and hyperoxia- exposed groups.

MAFIA mouse neonates received IP injections of AP20187 ligand on P1, P2, P3 and P7 and were exposed to normoxia versus hyperoxia for 10 days starting on P1. Whole lung homogenates were analyzed by flow cytometry. **A.** CSF1R-expressing cells depletion efficiency was assessed using flow cytometry with FITC-A laser to check for GFP reporter. GFP-positive cells were counted as a percentage in all cells (right graph). Data are presented as mean ± SEM (n = 3 in each group, *P* value was determined by t-test). **B.** Inflammatory cell populations were assessed using FACS analysis. Neutrophils were defined as $CD45^{+}$; $Gr\text{-}1^{+}$ cells; rAM as $CD11c^{+}$; $SiglecF^{+}$; $CD11b^{-}$; ExAM as $CD11c^{+}$; $CD11b^{+}$; $MHCII^{interm}$; dendritic cells (DCs) as $CD11c^{+}$; $CD11b^{+}$; $MHCII^{hi}$. **C.** Peripheral blood of hyperoxia exposed MAFIA pups was assessed for the presence of neutrophils ($CD45^{+}$; $Gr\text{-}1^{+}$). Representative flow cytometry plots are illustrated.

As expected, MAFIA pups exhibited a complete depletion of the rAM population in the normoxia-exposed group and no rAM in hyperoxia-exposed group (Fig. 8 B). Interestingly, there were clear populations of ExAM both in normoxia and hyperoxia-exposed groups and no neutrophil recruitment in response to hyperoxia. To examine whether neutrophils were depleted or their recruitment from the blood was abrogated, we check the peripheral blood of hyperoxia-exposed MAFIA pups for the presence of neutrophils and found that they were clearly present in the blood (Fig. 8 C). This finding demonstrates that in MAFIA mice neutrophil recruitment to the lung in response to hyperoxia injury was blocked.

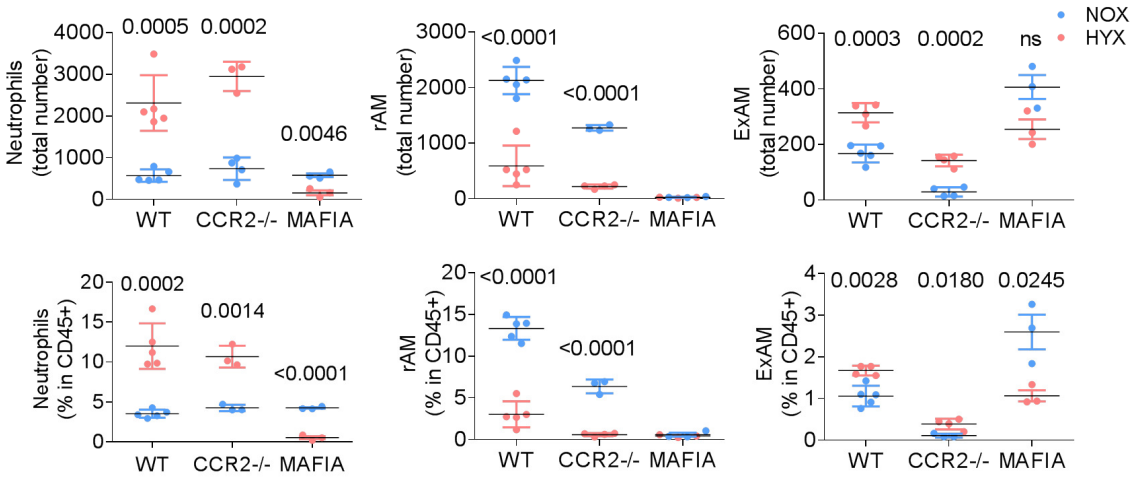

Figure 9 | Neutrophil, rAM and ExAM population analysis by flow cytometry.
Populations of neutriphils, rAM and ExAM were counted as a percentage it $CD45^+$ cells and as total numbers of cells for WT, CCR2 KO and MAFIA mice. Data are presented as mean ± SEM (n = 3-5 in each group, P values were determined by t-test).

4.4. ExAM of WT pups exposed to hyperoxia demonstrate a mixed population of M1- and M2-polarized cells, whereas MAFIA mice ExAM represent M2-polarized populations both in normoxia and hyperoxia exposed groups

Exudate alveolar macrophage populations of WT and MAFIA mice were analyzed for M1 and M2 polarization using flow cytometry analysis with CD40 and CD206, M1 and M2 polarization specific markers, respectively. It was found that ExAM population recruited to the lung of WT pups upon hyperoxia exposure represent a mixed population of M1- and M2-polarized macrophages (Fig. 10 A). Unlike WT,

MAFIA pups ExAM were found to be polarized to M2 anti-inflammatory phenotype both in normoxia and hyperoxia exposed groups (Fig. 10 B).

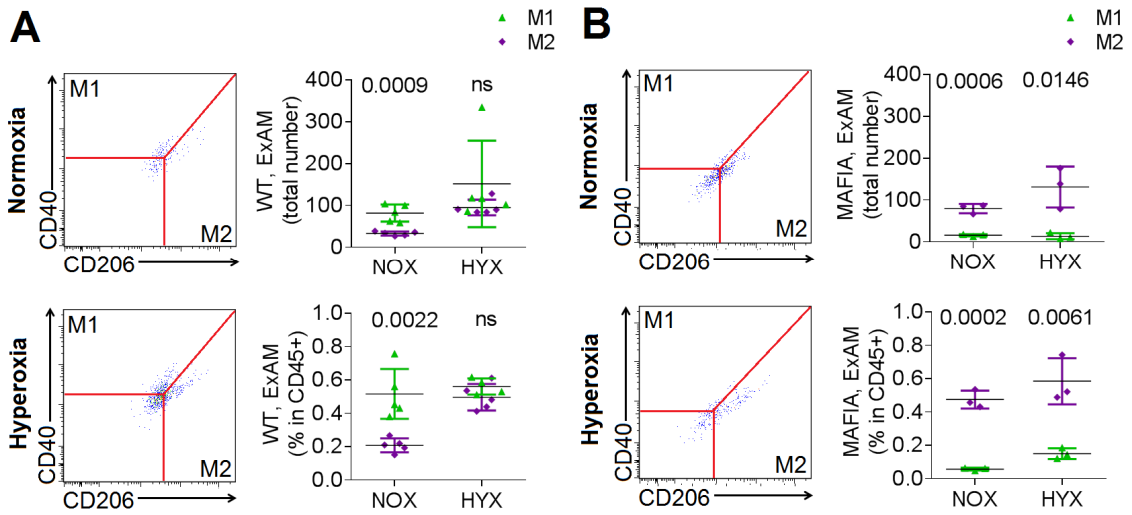

Figure 10 | Unlike WT, MAFIA pups ExAM are polarized to an M2 anti-inflammatory phenotype both in normoxia- and hyperoxia- exposed groups.

Whole-lung homogenates of WT and MAFIA pups exposed to normoxia or hyperoxia for 10 days were used for flow cytometry analysis and populations of ExAM ($CD45^+$; $CD11c^+$; $CD11b^+$; $MHCII^{interm}$) were analyzed for M1 and M2 polarization. M1-polarized macrophages were defined as $CD40^+$ and M2- as $CD206^+$. M1 and M2 populations are shown as total numbers and as percentages in $CD45^+$ cells (right panels) **A.** Wild type ExAM analyzed for CD40 and CD206 markers with flow cytometry analysis.

B. MAFIA pups ExAM analyzed for CD40 and CD206 markers with FACS analysis. Data are presented as mean ± SEM (n = 3-5 in each group, P values were determined by t-test). ns – not significant. Representative flow cytometry plots are illustrated.

Polarization of ExAM towards an M2 anti-inflammatory phenotype in MAFIA mice can be due to lack of neutrophils in the hyperoxia exposed pups.

4.5. MAFIA pups exposed to hyperoxia demonstrate a remarkable improvement of the lung structure

To check what effects CCR2 knockout and depletion of CSF1R-expressing cells have on the lung structure, stereological analysis was performed. Lungs of WT, CCR2 KO and MAFIA pups exposed to normoxia versus hyperoxia for 10 days were plastic embedded and analyzed using Visiopharm NewCast computer-assisted stereology system. In the hyperoxia-exposed group, CCR2 KO did not have an improvement of lung structure by visual examination, unlike MAFIA mice that had a clear

alveolarization improvement visual from the lung pictures (Fig. 11 A). Stereological analysis revealed that hyperoxia exposure leads to alveolarization arrest with fewer larger alveoli and thicker septa in WT pups, as it was expected. CCR2 KO pups had thicker septa in both normoxia and hyperoxia exposed groups and slight improvement in alveolar number in hyperoxia group as compared to WT normoxia (control) group. After analyzing the MAFIA groups, it was found that both septal wall thickness and alveolar numbers were improved and not statistically different from WT normoxia group (Fig. 11, Table 2).

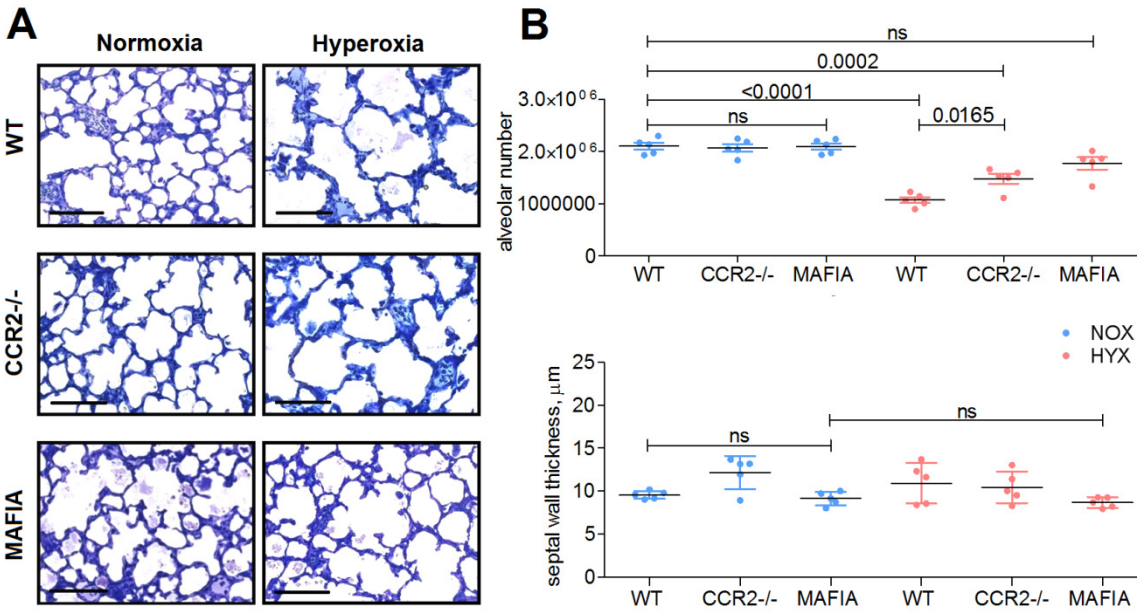

Figure 11 | Unlike CCR2 KO, MAFIA mice demonstrate a dramatic improvement of the lung structure in hyperoxia-exposed pups as compared with WT controls.

A. Representing pictures of WT, CCR2 KO and MAFIA pups lung structures. Lungs were plastic embedded, 2 µm sections were cut and stained with Richardson's stain. Scale bar 100 µm. **B.** Alveolar numbers and septal wall thickness counted on plastic embedded lungs using stereological analysis. Data are presented as mean ± SEM (n = 5 in each group, P values were determined by one-way ANOVA with a Tukey's post hoc test). ns – not significant.

These data demonstrate that the ExAM population does not play a crucial role in the arrested lung development observed in the BPD mouse model, and ExAM depletion alone does not lead to the significant improvement in lung structure. Depletion of CSF1R-expressing cells led to an almost full recovery of the lung structure in the hyperoxia treated group.

These findings demonstrate a pronounced role of CSF1R expressing cells and/or neutrophils in the arrested lung alveolarization and thickening of the septa observed in BPD.

Table 3 Structural parameters of WT, CCR2 KO and MAFIA pups exposed to normoxia or hyperoxia for 10 days

Parameter	Normoxia (21% O_2)				Hyperoxia (85% O_2)							
	WT	CCR2 KO	MAFIA	anti-Ly6G	WT		CCR2 KO		MAFIA		anti-Ly6G	
	mean ± S.E.	mean ± S.E.	mean ± S.E.	mean ± S.E.	mean ± S.E.	P value *versus* WT / 21% O_2	mean ± S.E.	P value *versus* WT / 21% O_2	mean ± S.E.	P value *versus* WT / 21% O_2	mean ± S.E.	P value *versus* WT / 21% O_2
$V_{(lung)}$ [cm^3]	0.164 ± 0.006	0.171 ± 0.001	0.174 ± 0.008	0.165 ± 0.005	0.186 ± 0.016	0.2551	0.172 ±0.012	0.3938	0.19 ±0.01	0.8438	0.17 ± 0.004	0.9997
CV [$V_{(lung)}$]	0.08	0.01	0.08	0.07	0.18		0.15		0.11		0.06	
$V_{V(par/lung)}$ [%]	89.88 ± 0.2	89.9 ± 0.5	88.8 ± 0.25	89.8 ± 0.17	91.36 ± 0.5	0.1254	90 ± 0.5	0.9999	89.9 ± 0.2	0.9999	89.85 ± 0.17	0.9999
$N_{(alv/par)}$ 10^6	2.1 ± 0.067	2.07 ± 0.071	2.096 ± 0.06	2.24 ± 0.121	1.07 ± 0.056	<0.0001	1.48 ± 0.95	0.0002	1.8 ± 0.11	0.0763	1.464 ± 0.146	0.0013
CV [$N_{(alv/par)}$]	0.06	0.07	0.07	0.1	0.1		0.13		0.12		0.2	
S_V [cm^{-1}]	720.5 ± 16.7	717.5 ± 17.8	681.9 ± 19.2	782.1 ± 26	444.6 ± 24.3	<0.0001	524.1 ± 15.3	<0.0001	540.0 ± 18.2	0.0002	530.9 ± 35.4	<0.0001
$S_{(sept/par)}$ [cm^2]	105.9 ± 2.9	110.3 ± 3.2	154.4 ± 6.9	117.9 ± 5	75.03 ± 6.47	0.0102	81.4 ± 6.8	0.0575	92.64 ± 7.35	0.5738	85.1 ± 3.3	0.1443
CV [$S_{(sept/par)}$]	0.06	0.06	0.07	0.09	0.17		0.17		0.16		0.08	
$V_{V(alv air)}$ [%]	65.6 ± 1.15	56.5 ± 2.7	69.6 ± 0.13	66.21 ± 2.5	76.04 ± 2	0.0072	72.84 ± 1.5	0.1328	76.68 ± 0.52	0.0037	72.89 ± 1.2	0.0993
$V_{V(alv air/lung)}$ [cm^3]	0.11 ± 0.006	0.097 ± 0.0045	0.1775 ± 0.003	0.11 ± 0.005	0.14 ± 0.013	0.0905	0.124 ± 0.008	0.7031	0.145 ± 0.007	0.0434	0.123 ± 0.0023	0.8250
CV [$V_{V(alv air/lung)}$]	0.1	0.1	0.1	0.1	0.19		0.13		0.11		0.04	
τ (sep) [µm]	9.536 ± 0.2	12.16 ± 0.86	9.1 ± 0.35	8.59 ± 0.4	10.9 ± 1	0.7125	10.44 ± 0.81	0.9310	8.66 ± 0.27	0.9410	9.43 ± 0.56	0.9999
CV [τ (sep)]	0.2	0.14	0.08	0.1	0.04		0.16		0.06		0.12	
l_m [µm]	36.57 ± 1.38	31.56 ± 1.5	39.21 ± 1	34.19 ± 2.5	69.24 ± 4.2	<0.0001	55.71 ± 1.36	<0.0001	57.08 ± 2.1	<0.0001	52.25 ± 1.57	0.0004
CV [l_m]	0.08	0.1	0.09	0.14	0.12		0.05		0.08		0.06	

V, volume; V_V, volume density; S, surface area; S_V, surface density; τ (sep), arithmetic mean septal thickness; N, number, CV, coefficient of variation; lm, mean linear intercept; par, parenchyma; alv air, alveolar airspaces; alv epi, alveolar epithelium; Alv, alveoli.
Values are presented as mean ± S.E, n=5 lungs per group. One-way ANOVA with Tukey's post-hoc analysis.

4.6. Neutrophil depletion leads to a mild improvement of the lung structure in hyperoxia-exposed WT pups

To determine whether neutrophil depletion alone can lead to an improved lung phenotype observed in MAFIA pups exposed to hyperoxia, neutrophils were depleted in WT pups by giving intraperitoneal injections of anti-Ly6G monoclonal antibody every second day starting on P1. Pups were exposed to normoxia or hyperoxia until P10 and depletion efficiency was controlled by flow cytometry. Flow cytometry analysis revealed that neutrophils were sufficiently depleted, rAM population was present in normoxia group and eliminated in hyperoxia group; and ExAM were recruited upon hyperoxia exposure (Fig. 12 A, B).

Exudate alveolar macrophages of neutrophil depleted pups were further analyzed for their M1/M2 polarization and it was found that in both groups (normoxia and hypeoxia) macrophages were polarized towards an M2 anti-inflammatory phenotype in the absence of neutrophils (Fig. 12 C) which goes along with the finding that ExAM are polarized to M2 phenotype in MAFIA pups (Fig. 10 B).

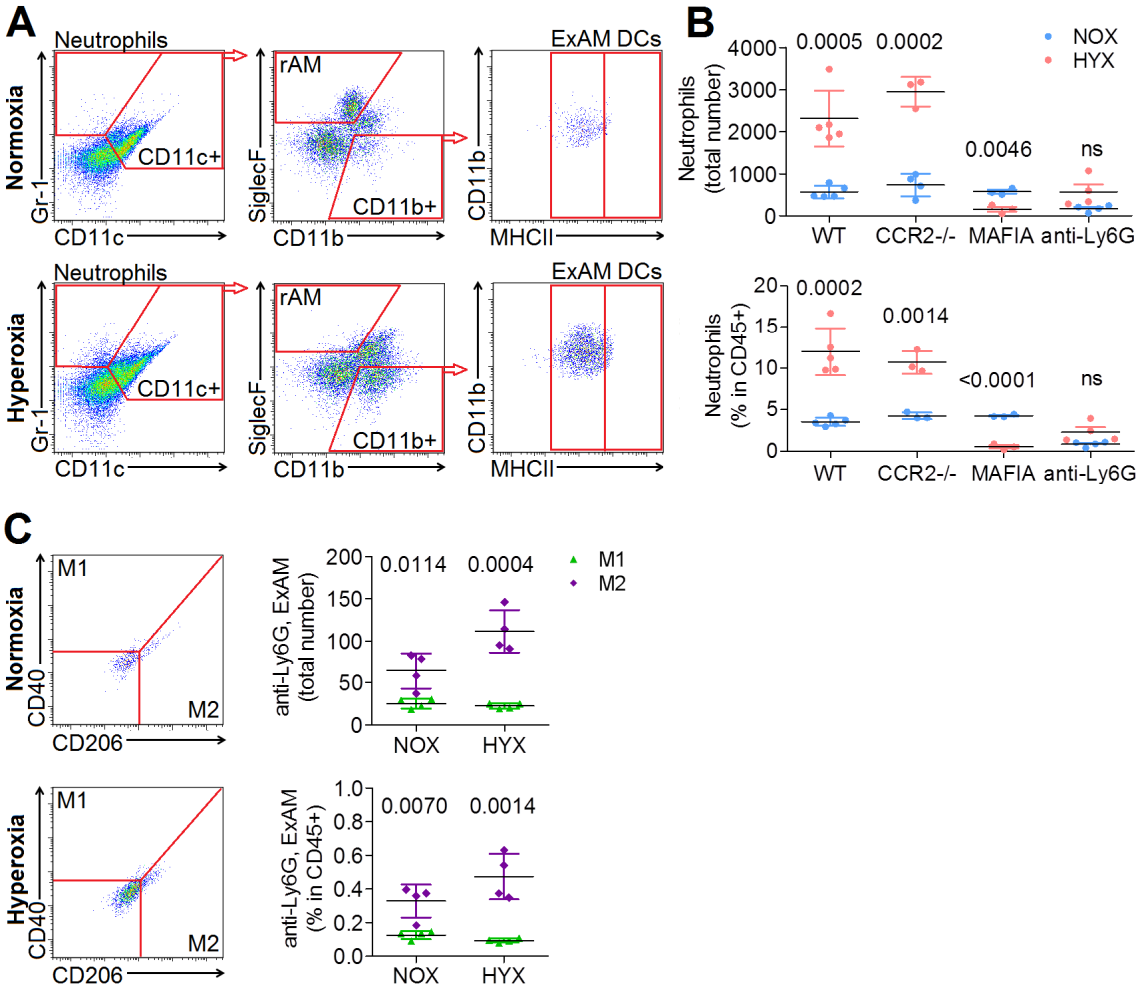

Figure 12 | Neutrophil depletion in mouse pups with an anti-Ly6G antibody demonstrates high depletion efficiency with ExAM polarization to M2 anti-inflammatory phenotype.

Neutrophils were depleted by giving intraperitoneal anti-Ly6G monoclonal antibody injections to WT pups every second day starting on P1. Pups were exposed to normoxia versus hyperoxia for 10 days and whole lung homogenates were used for flow cytometry. **A.** Flow cytometry analysis of inflammatory cell populations. Neutrophils were defined as $CD45^+$; $Gr\text{-}1^+$ cells; rAM as $CD11c^+$; $SiglecF^+$; $CD11b^-$; ExAM as $CD11c^+$; $CD11b^+$; $MHCII^{interm}$; dendritic cells (DCs) as $CD11c^+$; $CD11b^+$; $MHCII^{hi}$. **B.** Populations of neutriphils were counted as a percentage it $CD45^+$ cells and as total numbers of cells. **C.** ExAM populations were analyzed for M1 and M2 polarization using flow cytometry. M1-polarized macrophages were defined as $CD40^+$ and M2- as $CD206^+$. M1 and M2 populations are shown as total numbers and as percentages in $CD45^+$ cells (right panels). Data are presented as mean ± SEM (n = 3-5 in each group, *P* values were determined by t-test). ns – not significant. Representative flow cytometry plots are illustrated.

Analysis of the lung structure, however, revealed no obvious improvement of alveolarization with improved septal wall thickness (Fig. 13 A). Further precise stereological analysis of lung parameters revealed no significant alveolarization improvement in hyperoxia-exposed pups as compared with hyperoxia WT controls with

completely normal septal wall thickness (Fig. 13 B, Table 3). These data suggest that neutrophils may play a role in the thickening of alveolar wall in the progression of BPD, but neutrophil depletion alone is not enough to get a full lung structure improvement as it was observed in MAFIA mice.

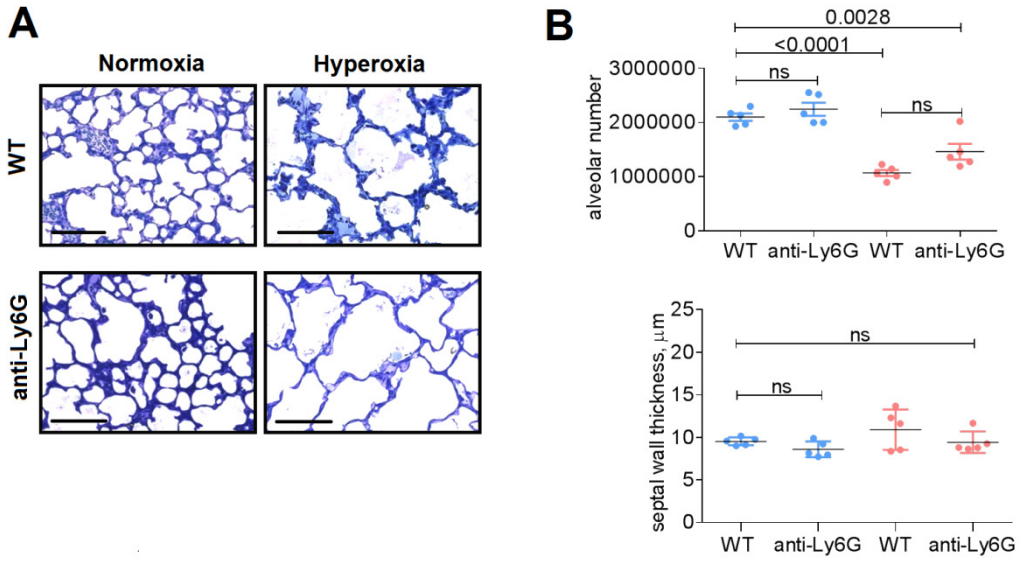

Figure 13 | Neutrophil depletion does not lead to improvement in alveolarization and improved alveolar septal thickness.

A. Lung structures of pups with neutrophil depletion 10 days after normoxia or hyperoxia exposure. Lungs were plastic embedded, 2 µm sections were cut and stained with Richardson's stain. Scale bar 100 µm. **B.** Septal wall thickness and alveolar numbers counted on plastic-embedded lungs using stereological analysis. Data are presented as mean ± SEM (n = 5 in each group, P values were determined by one-way ANOVA with a Tukey's post hoc test). ns – not significant.

This finding suggests that a population of CSF1R-expressing cells might play an important role in the arrested alveolarization associated with BPD.

Table 4 Structural parameters of wild type and neutrophil-depleted (anti-Ly6G) pups exposed to normoxia or hyperoxia for 10 days

Parameter	Normoxia (21% O_2)		Hyperoxia (85% O_2)			
	WT	anti-Ly6G	WT		anti-Ly6G	
	mean ± S.E.	mean ± S.E.	mean ± S.E.	P value *versus* WT / 21% O_2	mean ± S.E.	P value *versus* WT / 21% O_2
$V_{(lung)}$ [cm^3]	0.164 ± 0.006	0.165 ± 0.005	0.186 ± 0.016	0.2551	0.17 ± 0.004	0.9997
CV [$V_{(lung)}$]	0.08	0.07	0.18		0.06	
$V_{V(par/lung)}$ [%]	89.88 ± 0.2	89.8 ± 0.17	91.36 ± 0.5	0.1254	89.85 ± 0.17	0.9999
$N_{(alv/par)}$ 10^6	2.1 ± 0.067	2.24 ± 0.121	1.07 ± 0.056	<0.0001	1.464 ± 0.146	0.0013
CV [$N_{(alv/par)}$]	0.06	0.1	0.1		0.2	
S_V [cm^{-1}]	720.5 ± 16.7	782.1 ± 26	444.6 ± 24.3	<0.0001	530.9 ± 35.4	<0.0001
$S_{(sept/par)}$ [cm^2]	105.9 ± 2.9	117.9 ± 5	75.03 ± 6.47	0.0102	85.1 ± 3.3	0.1443
CV [$S_{(sept/par)}$]	0.06	0.09	0.17		0.08	
$V_{V(alv air)}$ [%]	65.6 ± 1.15	66.21 ± 2.5	76.04 ± 2	0.0072	72.89 ± 1.2	0.0993
$V_{V(alv air/lung)}$ [cm^3]	0.11 ± 0.006	0.11 ± 0.005	0.14 ± 0.013	0.0905	0.123 ± 0.0023	0.8250
CV [$V_{V(alv air/lung)}$]	0.1	0.1	0.19		0.04	
τ (sep) [μm]	9.536 ± 0.2	8.59 ± 0.4	10.9 ± 1	0.7125	9.43 ± 0.56	0.9999
CV [τ (sep)]	0.2	0.1	0.04		0.12	
l_m [μm]	36.57 ± 1.38	34.19 ± 2.5	69.24 ± 4.2	<0.0001	52.25 ± 1.57	0.0004
CV [l_m]	0.08	0.14	0.12		0.06	

V, volume; V_V, volume density; S, surface area; S_V, surface density; τ (sep), arithmetic mean septal thickness; N, number, CV, coefficient of variation; lm, mean linear intercept; par, parenchyma; alv air, alveolar airspaces; alv epi, alveolar epithelium; Alv, alveoli. Values are presented as mean ± S.E, n=5 lungs per group. One-way ANOVA with Tukey's post-hoc analysis.

4.7. Cell population (Pop3) might play a role in the development of BPD

As long as MAFIA mice exposed to hyperoxia demonstrate such a clear lung structure improvement; and neutrophil depletion alone did not lead to any improvement in alveolarization, some other cell population that was depleted in MAFIA mice must play an important role in the alveolarization block.

To examine whether another cell population that was depleted in MAFIA mice could play a role in the great lung improvement observed in hyperoxia group, three populations of cells that were not included in the initial analysis were examined. In Fig. 14 A representative flow cytometry plots of WT pups exposed to normoxia and hyperoxia are illustrated and these three populations are marked as Pop1, Pop2 and Pop3. Already from the flow cytometry plots it is clear that Pop3 is significantly increased in size in hyperoxia-exposed group. Examination of all three populations on side and forward scatter revealed that, unlike Pop1 and Pop2, Pop3, clearly represents granulocytes (Fig. 14 B).

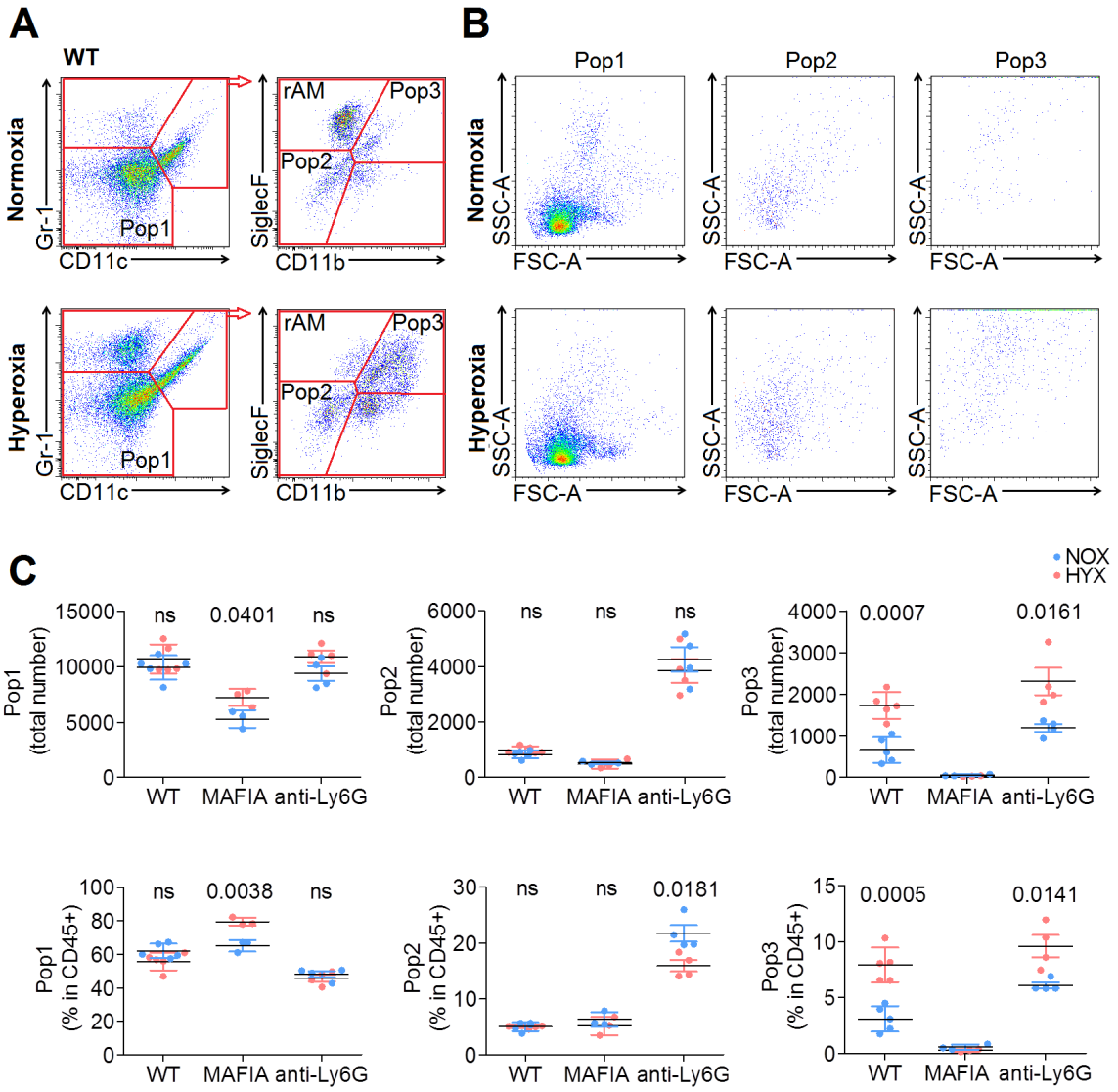

Figure 14 | Pop3 consists of granulocytes, is increased upon hyperoxia exposure both in wild type and neutrophil depleted pups, and is completely depleted in MAFIA pups.

A. Representative flow cytometry plots of wild type pups exposed to normoxia versus hyperoxia for 10 days illustrating three populations of cells (Pop1, Pop2 and Pop3) initially not included in the analysis. **B.** Side- and forward-scatter plots of Pop1, Pop2 and Pop3 in normoxia and hyperoxia exposed WT pups. **C.** Pop1, Pop2 and Pop3 cell populations were counted as total numbers and as a percentage in $CD45^+$ cells in WT, MAFIA and neutrophil depleted pups exposed to normoxia versus hyperoxia for 10 days. Data are presented as mean ± SEM (n = 3-5 in each group, P values were determined by t-test). ns – not significant.

To determine which population is expanded upon hyperoxia exposure, cell numbers of Pop1, Pop2 and Pop3 were calculated for WT and neutrophil-depleted mice and compared with MAFIA pups (Fig. 14 C). It became clear that Pop3 is the only population completely depleted in MAFIA mice and in the same time significantly

increased in size in both WT and neutrophil depleted pups upon hyperoxia exposure (Fig. 14 C). These observations suggest that Pop3 might play an important role in the lung alveolarization arrest observed in both WT and neutrophil depleted pups exposed to hyperoxia.

To further analyze Pop1, Pop2 and Pop3, all three populations were FACS sorted and cytospin followed by H&E staining was performed. It was found that Pop1 and Pop2 consist of small round cells with large nuclei characteristic of lymphocytes and monocytes, whereas Pop3 appeared to be a population of cells with macrophage-like charachteristics (Fig. 15).

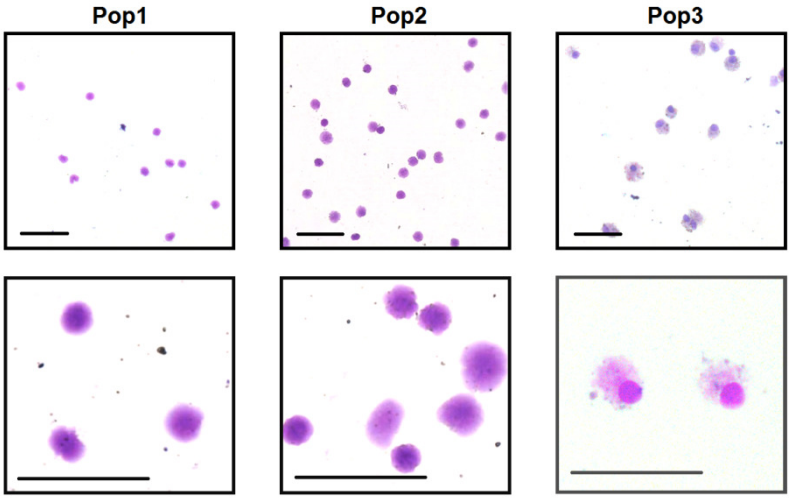

Figure 15 | Pop3 represents a population of macrophage-like cells, unlike Pop1 and Pop2.
FACS sorting of Pop1, Pop2 and Pop3 was performed followed by cytospin and H&E staining for WT and neutrophils depleted pups exposed to hyperoxia for 10 days. Representative pictures are illustrated. Scale bar 50 μm.

Pop3 was further examined for the level of MHCII expression using FACS analysis and it was found that Pop3 is highly MHCII enriched (Fig. 16 A). This finding together with macrophage-like phenotype of Pop3 led us to an idea that Pop3 can be in fact population of resident alveolar macrophages (rAM) that changed phenotype upon hyperoxia exposure and became $CD11b^{+}$ and $MHCII^{high}$.

4.8. rAM change phenotype upon hyperoxia exposure

To verify if Pop3 can be a population of resident alveolar macrophages (rAM) that changed its phenotype upon hyperoxia exposure, we compared total numbers of these two populations summaries (rAM + Pop3) in normoxia and hyperoxia exposed

pups of WT and neutrophil depleted groups and found that these numbers are exactly the same (Fig. 16 B).

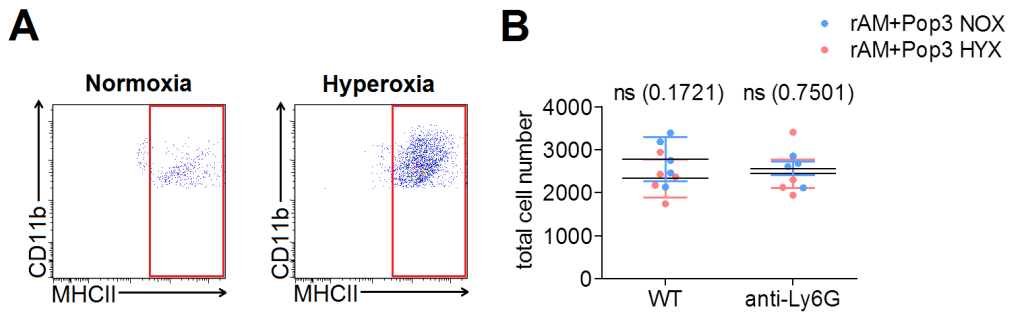

Figure 16 | rAM change phenotype upon hyperoxia exposure.

A. Flow cytometry analysis of Pop3 from P10 WT pups exposed to normoxia or hyperoxia demonstrating that Pop3 cells are highly MHCII expressing. **B.** Total cell numbers summary of rAM and Pop3 populations was counted for WT and neutrophil depleted (anti-Ly6G) pups exposed to normoxia or hyperoxia for 10 days. Data are presented as mean ± SEM (n = 4-5 in each group, P values were determined by t-test), ns – not significant.

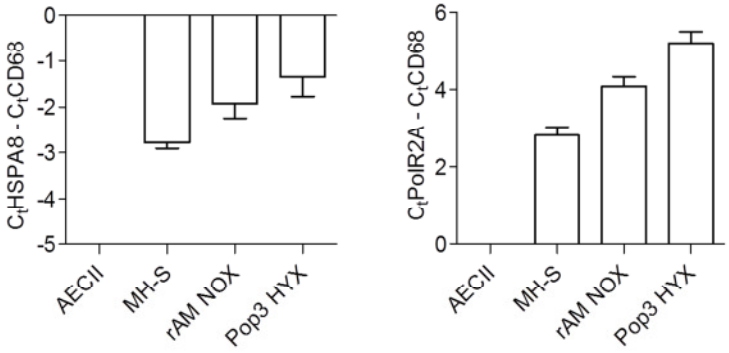

Figure 17 | Pop3 represents population ofmacrophages.

Resident alveolar macrophages population of normoxia-exposed pups and Pop3 of hyperoxia-exposed pups were FACS sorted and rtPCR analysis with CD68 macrophage-specific marker was performed. PolR2A and HSPA8 were used as reference genes. Primary type II cells (AECII) and MH-S cell line mRNA were used as negative and positive controls, respectively. Data are presented as mean ± SEM (n = 4 in each group).

To make sure that Pop3 represents a population of macrophages, Pop3 and rAM populations were FACS sorted, total mRNA was isolated and a real-time quantitative PCR analysis was performed with CD68 macrophage-specific primers. Two reference genes were used (HSPA8 and PolR2A). Total mRNA of mouse alveolar macrophages cell line (MH-S) was used as positive control and total mRNA of primary type two cells

(AECII) as negative control (Fig. 17). It was found that Pop3 expresses high levels of CD68, comparable with rAM population and MH-S cell line, which clearly proves that Pop3 represents a population of macrophages.

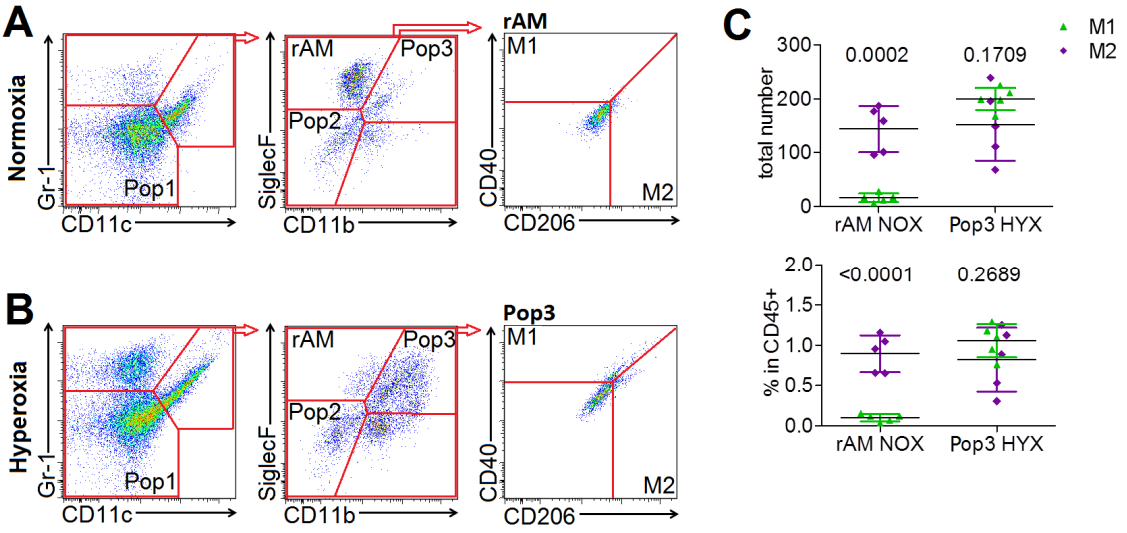

Figure 18 | In normoxia-exposed mouse pups rAM polarize towards an M2 phenotype while hyperoxia-exposed group represent a mixed population of M1- and M2-polarized cells (Pop3).
A. Resident alveolar macrophage population of WT normoxia-exposed mice was analyzed for M1/M2 polarization using CD40 and CD106 markers. M1-polarized macrophages were defined as $CD40^+$ and M2- as $CD206^+$. **B.** WT Pop3 population in hyperoxia group was analyzed for M1/M2 polarization using CD40 and CD206 markers. M1-polarized macrophages were defined as $CD40^+$ and M2- as $CD206^+$. **C.** M1 and M2 populations are counted as total numbers and as percentages in $CD45^+$ cells. Data are presented as mean ± SEM (n = 5 in each group, *P* values were determined by t-test). Representative flow cytometry plots are illustrated.

Resident alveolar macrophages of WT normoxia groups were analyzed for polarization and it was found that resident macrophages have a tendency to polarize towards M2 anti-inflammatory phenotype with however vast majority of macrophages not polarized at all (Fig. 18 A, C). After exposing pups to hyperoxia for 10 days, Pop3 was also analyzed for polarization and revealed a mixed population of M1- and M2-polarized macrophages (Fig. 18 B, C).

All these findings suggest that a population of resident alveolar macrophages (rAM) changes phenotype upon hyperoxia exposure and starts expressing CD11b and MHCII receptors that are characteristic of activated immune cells. Resident macrophages also represent a mixed popupation of M1- and M2-polarized cells like exudate macrophages in hyperoxia group. This population of activated rAM together

with recruited neutrophils can harm the lung and lead to arrested alveolarization with thicker alveolar wall.

5. Discussion

Macrophages are present in large numbers in all developing organs and key periods of organogenesis correlate with maximum macrophage numbers (Cecchini et al. 1994). In normal organ development, tissue remodeling is achieved through cells apoptosis followed by cellular debris phagocytic clearance performed by macrophages that are in the same time potent effector cells producing a range of growth factors that regulate cellular differentiation and promote angiogenesis (Stefater et al. 2011).Tissue macrophage-deficient mice have a range of developmental abnormalities, including impaired growth and fertility (Dai et al. 2002, Wiktor-Jedrzejczak et al. 1990, Yoshida et al. 1990). It is known that macrophages are essential in the normal pancreas, mammary gland and kidney development, organs that like the lung develop through branching morphogenesis. In normal development macrophages are localized around developing terminal buds and their absence leads to branching abnormalities with poorly branched terminal buds in the mammary gland (Gouon-Evans et al. 2000, Ingman et al. 2006),and abnormal islet cell morphology in the pancreas (Banaei-Bouchareb et al. 2004, Banaei-Bouchareb et al. 2006). However, less is known about the role of macrophages in the developing of the lung.

Macrophages are abundant in developing embryonic lung and are localized in mesenchymal tissue surrounding alveolar buds, in particular within branch points (Fig. 18 A). Macrophages seeding of the lung tissue starts shortly after birth, as was demonstrated with SiglecF alveolar macrophages specific marker staining (Fig. 18 B). Alveolar macrophage number is increased during alveolarization and display an M2 anti-inflammatory polarization phenotype (Jones C. V. et al. 2013). As long as alveolar macrophages play an important role in lung development, any change in their phenotype and expression profile may have a serious impact on the lung structure.

In this study we were aimed to investigate the roles of different inflammatory cell populations in the arrested lung development and thickening of the septal wall observed in BPD. In WT pups exposed to hyperoxia for 10 days neutrophils (Gr-1^{+}) and ExAM (CD11b^{+}) are massively recruited to the lung and rAM population (Siglec^{+}, CD11b^{-}) is eliminated. First, to check the role of ExAM (inflammatory CCR2^{hi} macrophages recruited to the sites of inflammation) we used CCR2 KO mouse to abrogate the ExAM recruitment to the lung upon hyperoxia exposure. Lung structure analysis revealed that abrogation of ExAM recruitment to the lung leads to a mild

improvement in alveolarization and no septal wall improvement of the lung, demonstrating that other cell types must play a crucial role in the arrested lung development and septal thickening of the lung associated with BPD (Fig. 11, Table 2).

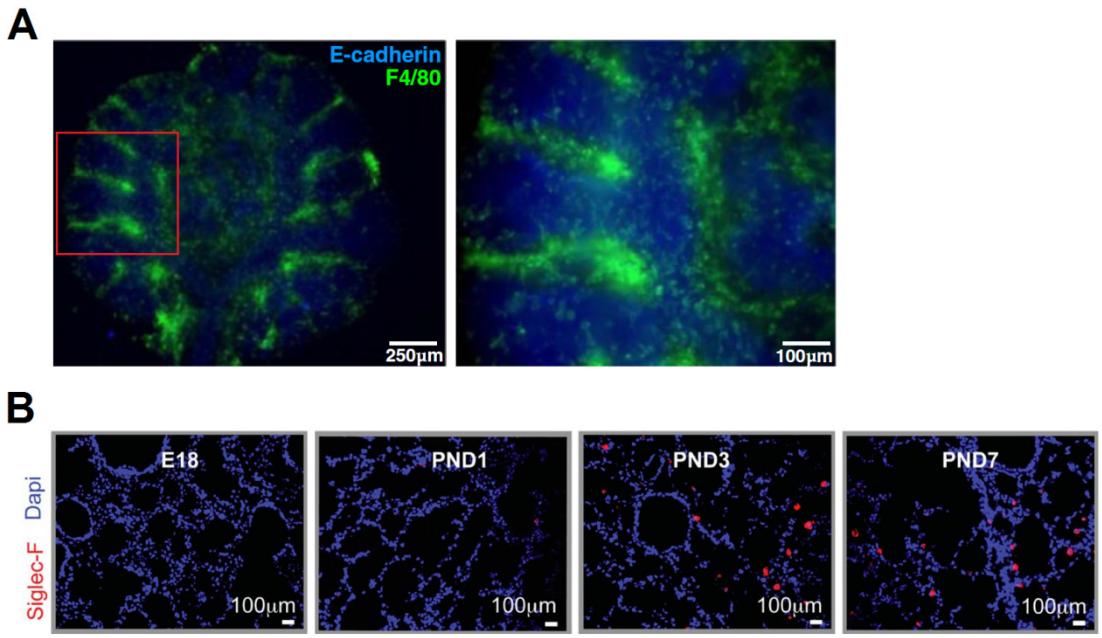

Figure 19 | Alveolar macrophages are localized in mesenchymal tissue in the developing embryonic mouse lung and start seeding alveolar spaces only after the birth.

A. Immunofluorescence labelling of the E12.5 embryonic mouse lung epithelium (anti-E-cadherin; blue) and macrophages (anti-F4/80; green). Modified from (Jones C. V. et al. 2013). **B.** Cryosection of mouse lungs stained with DAPI (blue) and SiglecF (red). Modified from (Guilliams et al. 2013). PND-postnatal day

To assess the role of CSF1R-expressing cells in the development of BPD-like phenotype, we exposed MAFIA pups that have a suicide gene under control of CSF1R, to hyperoxia for 10 days and found that population of rAM was completely depleted in these pups and recruitment of neutrophils from the blood was completely blocked, but ExAM were present in the lung of both normoxia and hyperoxia groups. Further analysis of ExAM polarization revealed that exudate macrophages had M2 anti-inflammatory phenotype. It is not known if the origin of these ExAM populations, but it can be that these are the cells that avoided depletion as its efficiency is not more than 85%. Lung structure analysis of MAFIA pups demonstrated almost normal lung structure in hyperoxia exposed group with normal septal wall thickness and greatly improved alveolarization (Fig. 11, Table 2). These data suggest that either neutrophils

or some CSF1R^{hi} population of inflammatory cells must play a role in the alveolarization arrest and septal wall thickening.

To examine the role of neutrophils in the development of a BPD-like phenotype, neutrophils were depleted by giving intraperitoneal injection of anti-Ly6G antibody to the neonate WT pups and it was found that in the absence of neutrophils, ExAM were recruited to the lung and had M2 phenotype. But, analysis of the lung structures did not reveal any significant alveolarization improvement in hyperoxia-exposed group with yet completely improved septal wall thickness. From these findings it was concluded that neutrophils play a role in the thickening of the septal wall, but almost do not contribute to the disrupted alveolarization.

Altogether these findings demonstrate that some CSF1R^{hi} population depleted in MAFIA mice has a great effect on alveolarization. After examination of WT controls, neutrophils depleted pups and MAFIA pups exposed to normoxia versus hyperoxia, it was found that there is a distinct SiglecF^{hi}, CD11b^{hi}, MHCII^{hi} population (Pop3) that increases in size in hyperoxia groups of WT and neutrophil-depleted mice, whereas it is completely depleted in MAFIA pups. Examination of Pop3 population using cytospin revealed macrophage-like phenotype of these cells that led to an idea that this population can be in fact rAM population that changes phenotype upon hyperoxia exposure (Fig. 14, 15). Absolute numbers comparison of rAM+Pop3 of hyperoxia- and normoxia-exposed WT and neutrophil-depleted pups revealed that rAM+Pop3 numbers are the same in normoxia- and hyperoxia-exposed mice (Fig. 16). Further, rAM and Pop3 populations were FACS sorted, total mRNA was isolated followed by real time quantitative PCR with CD68 macrophage-specific primers and it was found that Pop3 expresses similar levels of CD68 as rAM population that proves macrophage nature of Pop3 (Fig. 17). These findings support the idea that rAM change phenotype upon hyperoxia exposure and shift to CD11b^{+} side on the flow cytometry plot.

If that is the case, Pop3 cells can be polarized towards M1 or M2 phenotype. Resident macrophages of WT normoxia group were compared with Pop3 cells of WT hyperoxia group and it was found that in normoxia group rAM polarize towards M2 anti-inflammatory phenotype, as described in the literature (Jones C. V. et al. 2013) and Pop3 represents a mixed population of M1- and M2-polarized cells in hyperoxia group (Fig. 18) and can therefore certainly contribute to the disruption of the lung structure.

When studying the damage and deregulation of the neonatal lung associated with preterm birth, the impact of inflammation on macrophage populations should be

considered. Diversity and plasticity are hallmarks of monocyte-macrophage lineage cells and M1 or M2 activation states represent extremes of a continuum of activation states. In tissues macrophages respond to environmental signals such as damaged cells or activated lymphocytes with the acquisition of distinct functional phenotypes. Pathology is frequently associated with dynamic changes in macrophage activation, with classically M1-polarizedmacrophages implicated in initiating and sustaining inflammation and M2-polarized macrophages associated with chronic inflammation resolution (Gordon and Martinez 2010, Martinez et al. 2009). Macrophages responsiveness to exogenous stimulus such as hyperoxia can also depend on the developmental stage of macrophages. For example, preterm rabbit alveolar macrophages exposed to hyperoxia overnight start expressing inflammatory cytokines such as IL-1β and IL-8, unlike term alveolar macrophages exposed to hyperoxia (Rozycki et al. 2002).

We believe that under normal physiological conditions without any external stimulus resident alveolar macrophages ($SiglecF^{+}$; $CD11b^{-}$) maintain tissue homeostasis, remove aged or dead cells and toxic molecules. After hyperoxia exposure, activated M1-polarized resident alveolar macrophages produce high reactive oxygen and nitrogen intermediates and secrete many pro-inflammatory cytokines which promote other phagocytic cells recruitment, such as neutrophils and dendritic cells to exaggerate the killing capabilities of pathogens; and such resident macrophage activation and subsequent massive neutrophil recruitment leads to an arrested alveolarization and normal lung development disruption in neonates.

Summary

Bronchopulmonary dysplasia (BPD) is a chronic lung disease of infants born extremely preterm and characterized by inflammation and simplification of the distal lung structure with fewer, larger alveoli. A number of studies have demonstrated elevated macrophage and neutrophil numbers in the diseased lung, and it is becoming apparent that there is a connection between impaired alveolarization and the preceding inflammatory process. As macrophages play key role in tissue remodeling, lung injury and repair, we focused on the role of macrophages in the pathogenesis of BPD.

Using a mouse model of BPD that relies on hyperoxia (HYX) and two transgenic mouse lines (CCR2 KO and MAFIA (Macrophage Fas-Induced Apoptosis)) functional roles of different alveolar macrophages (AM), namely resident (rAM) and exudate (ExAM) were studied. It was found that WT mice had a population of rAM ($CD11c^+/SiglecF^+/CD11b^-$) in NOX group which was gone in HYX-exposed mice; and recruitment of neutrophils ($Gr\text{-}1^+$) and ExAM ($CD11c^+/CD11b^+/MHCII^{interm}$) upon HYX exposure. CCR2 KO mice had neutrophil recruited upon HYX exposure, but no ExAM recruitment. MAFIA mice lacked rAM populations in NOX, had no influx of neutrophils in HYX, but had clear populations of ExAM both in NOX and HYX groups. Lung structures analysis revealed that WT mice had 2.1 ± 0.067 million alveoli and a septa of 9.53 ± 0.2 μm in NOX group and reduced alveolar number (1.07 ± 0.056 million) and thicker septa (10.90 ± 1.0 μm) in HYX-exposed mice. CCR2 KO mice had a small alveolarization improvement (1.48 ± 0.95 million) in HYX group and no septal thickness improvement, whereas MAFIA mice had a great improvement in the lung structure of HYX exposed pups (1.8 ± 0.11 million alveoli and 8.66 ± 0.27 μm septa). No alveolar number improvement after depleting neutrophils alone in HYX-exposed WT mice, was observed. Further analysis showed that a population of $CD11c^+/SiglecF^+/CD11b^+/MHCII^{high}$ cells (Pop3) was significantly increased in WT and neutrophil-depleted mice upon HYX exposure and completely depleted in MAFIA mice. Pop3 sorting followed by cytospin and H&E staining and rtPCR analysis with CD68-specific primers demonstrated that Pop3 is a population of macrophages.

These data suggest a novel role of rAM in the development of BPD and demonstrates that rAM might change phenotype upon HYX exposure and this population of activated macrophages ($SiglecF^+/CD11b^+/MHCII^{high}$) might contribute greatly to the alveolarization arrest observed in BPD.

Zusammenfassung

Die Bronchopulmonale Dysplasie (BPD) ist eine chronische Lungenerkrankung bei extrem frühgeborenen Kindern. Sie ist durch Inflammation und Rarefizierung der distalen Lungenstrukturen mit verminderten und vergrößerten Alveoli gekennzeichnet. Zahlreiche Studien haben gezeigt, dass eine erhöhte Anzahl von Makrophagen und Neutrophilen in der erkrankten Lunge vorliegt. Ausserdem besteht offensichtlich eine Verbindung zwischen der eingeschränkten Alveolarisation und dem ihr vorangehenden Inflammationsprozess. In unserer Studie fokussieren wir uns auf die Rolle der Makrophagen in der Pathogenese der BPD, da Makrophagen eine Schlüsselrolle im Gewebe-Remodelling, bei der Lungenschädigung und der Regeneration spielen.

Unter Verwendung eines BPD-Mausmodells mit Hilfe von Hyperoxie (HYX) und zwei transgenen Mauslinien (CCR2 KO und MAFIA (Makrophage FAS-induzierte Apoptose)) haben wir die funktionelle Bedeutung verschiedener Populationen von residenten (rAM) und exsudaten Alveolarmakrophagen (ExAM) untersucht. Wir zeigten, dass WT Kontrollmäuse der Normoxiegruppe (NOX) eine Population von rAM ($CD11c^+/SiglecF^+/CD11b^-$) aufweisen, die in der Hyperoxiegruppe nicht mehr nachweisbar ist. Ausserdem war eine Rekrutierung von Neutrophilen ($CD45^+/Gr\text{-}1^+$) und ExAM ($CD11c^+/CD11b^+/MHCII^{interm}$) unter Hyperoxie zu verzeichnen. CCR2 KO Mäuse rekrutieren Neutrophile unter Hyperoxie, jedoch rekrutieren sie keine ExAM. Im Vergleich dazu fehlte bei den MAFIA Mäusen die rAM Population in Normoxie sowie der Influx von Neutrophilen in Hyperoxie, aber es zeigte sich eine eindeutige Population von ExAM sowohl in der Normoxie- als auch in der Hyperoxiegruppe. Die Analysen der Lungenstruktur zeigten, dass WT Mäuse der Normoxiegruppe 2,1 ± 0,067 Mio. Alveoli und eine Septendicke von 9,53 ± 0,2 µm aufweisen, während in der Hyperoxiegruppe eine reduzierte Anzahl von Alveoli (1,07 ± 0,056 Mio.) und dickere Septen (10,9 ± 1,0 µm) zu beobachten war. CCR2 KO Mäuse weisen eine geringe Verbesserung der Alveolarisation (1,48 ± 0,95 Mio.) in der Hyperoxiegruppe auf, zeigten jedoch keine Verbesserung der Septendicke. Im Gegensatz dazu war eine enorme Verbesserung der Lungenstruktur bei den MAFIA Mäusen der Hyperoxiegruppe festzustellen (1,8 ± 0,11 Mio. Alveoli und 8,66 ± 0,27 µm Septen). Nach der Depletion von Neutrophilen in WT Mäusen der Hyperoxiegruppe war keine Verbesserung der Alveolenanzahl zu verzeichnen. Weitere Analysen zeigten eine

signifikant erhöhte $CD11c^+/SiglecF^+/CD11b^+/MHCII^{high}$ Population (Pop3) sowohl in WT Mäusen als auch in den Neutrophilen-depletierten Mäusen der Hyperoxiegruppe; bei den MAFIA Mäusen war im Gegensatz dazu keine zu verzeichnen. Das Sortieren von Pop3 mit anschließendem Cytospin, H&E Färbung und rtPCR Analyse mit CD68 spezifischen Primern ergab, dass es sich bei Pop3 wie bei rAM um eine Makrophagenpopulation handelt.

Die vorliegenden Daten legen nahe, dass rAM eine Rolle in der Entwicklung von BPD spielen könnte. Desweiteren deuten sie darauf hin, dass rAM unter Hyperoxie ihren Phänotyp ändern könnte und dass diese Population von aktivierten Makrophagen ($SiglecF^+/CD11b^+/MHCII^{high}$) möglicherweise entscheidend zum Stillstand der Alveolarisation, wie sie bei der BPD zu verzeichnen ist, beitragen könnte.

Literature

Aghai ZH, Saslow JG, Mody K, Eydelman R, Bhat V, Stahl G, Pyon K, Bhandari V. 2013. IFN-gamma and IP-10 in tracheal aspirates from premature infants: relationship with bronchopulmonary dysplasia. Pediatr Pulmonol 48:8-13.

Ajami B, Bennett JL, Krieger C, Tetzlaff W, Rossi FM. 2007. Local self-renewal can sustain CNS microglia maintenance and function throughout adult life. Nat Neurosci 10:1538-1543.

Albertine KH, Jones GP, Starcher BC, Bohnsack JF, Davis PL, Cho SC, Carlton DP, Bland RD. 1999. Chronic lung injury in preterm lambs. Disordered respiratory tract development. Am J Respir Crit Care Med 159:945-958.

Alvira CM, Abate A, Yang G, Dennery PA, Rabinovitch M. 2007. Nuclear factor-kappaB activation in neonatal mouse lung protects against lipopolysaccharide-induced inflammation. Am J Respir Crit Care Med 175:805-815.

Ambalavanan N, Carlo WA, D'Angio CT, McDonald SA, Das A, Schendel D, Thorsen P, Higgins RD. 2009. Cytokines associated with bronchopulmonary dysplasia or death in extremely low birth weight infants. Pediatrics 123:1132-1141.

Ancuta P, Rao R, Moses A, Mehle A, Shaw SK, Luscinskas FW, Gabuzda D. 2003. Fractalkine preferentially mediates arrest and migration of $CD16^+$ monocytes. J Exp Med 197:1701-1707.

Anyanwu AC, Bentley JK, Popova AP, Malas O, Alghanem H, Goldsmith AM, Hershenson MB, Pinsky DJ. 2014. Suppression of inflammatory cell trafficking and alveolar simplification by the heme oxygenase-1 product carbon monoxide. Am J Physiol Lung Cell Mol Physiol 306:14.

Arnold L, Henry A, Poron F, Baba-Amer Y, van Rooijen N, Plonquet A, Gherardi RK, Chazaud B. 2007. Inflammatory monocytes recruited after skeletal muscle injury switch into antiinflammatory macrophages to support myogenesis. J Exp Med 204:1057-1069.

Auten RL, Jr., Mason SN, Tanaka DT, Welty-Wolf K, Whorton MH. 2001. Anti-neutrophil chemokine preserves alveolar development in hyperoxia-exposed newborn rats. Am J Physiol Lung Cell Mol Physiol 281:L336-344.

Bagchi A, Viscardi RM, Taciak V, Ensor JE, McCrea KA, Hasday JD. 1994. Increased activity of interleukin-6 but not tumor necrosis factor-alpha in lung lavage of

premature infants is associated with the development of bronchopulmonary dysplasia. Pediatr Res 36:244-252.

Banaei-Bouchareb L, Gouon-Evans V, Samara-Boustani D, Castellotti MC, Czernichow P, Pollard JW, Polak M. 2004. Insulin cell mass is altered in Csf1op/Csf1op macrophage-deficient mice. J Leukoc Biol 76:359-367.

Banaei-Bouchareb L, Peuchmaur M, Czernichow P, Polak M. 2006. A transient microenvironment loaded mainly with macrophages in the early developing human pancreas. J Endocrinol 188:467-480.

Bancalari E, Abdenour GE, Feller R, Gannon J. 1979. Bronchopulmonary dysplasia: clinical presentation. J Pediatr 95:819-823.

Baraldi E, Filippone M. 2007. Chronic lung disease after premature birth. N Engl J Med 357:1946-1955.

Berger J, Bhandari V. 2014. Animal models of bronchopulmonary dysplasia. The term mouse models. Am J Physiol Lung Cell Mol Physiol 307:10.

Bhandari A, Bhandari V. 2009. Pitfalls, problems, and progress in bronchopulmonary dysplasia. Pediatrics 123:1562-1573.

Bhandari V. 2014. Postnatal inflammation in the pathogenesis of bronchopulmonary dysplasia. Birth Defects Res A Clin Mol Teratol 100:189-201.

Bhandari V, Gruen JR. 2006. The genetics of bronchopulmonary dysplasia. Semin Perinatol 30:185-191.

Biswas SK, Mantovani A. 2010. Macrophage plasticity and interaction with lymphocyte subsets: cancer as a paradigm. Nat Immunol 11:889-896.

Bland RD, Ertsey R, Mokres LM, Xu L, Jacobson BE, Jiang S, Alvira CM, Rabinovitch M, Shinwell ES, Dixit A. Mechanical ventilation uncouples synthesis and assembly of elastin and increases apoptosis in lungs of newborn mice. Prelude to defective alveolar septation during lung development? Am J Physiol Lung Cell Mol Physiol. 2008 Jan;294(1):L3-14. Epub 2007 Oct 12.

Boring L, Gosling J, Chensue SW, Kunkel SL, Farese RV, Jr., Broxmeyer HE, Charo IF. 1997. Impaired monocyte migration and reduced type 1 (Th1) cytokine responses in C-C chemokine receptor 2 knockout mice. J Clin Invest 100:2552-2561.

Bose CL, Dammann CE, Laughon MM. 2008. Bronchopulmonary dysplasia and inflammatory biomarkers in the premature neonate. Arch Dis Child Fetal Neonatal Ed 93:1.

Botet F, Figueras-Aloy J, Miracle-Echegoyen X, Rodriguez-Miguelez JM, Salvia-Roiges MD, Carbonell-Estrany X. 2012. Trends in survival among extremely-low-birth-weight infants (less than 1000 g) without significant bronchopulmonary dysplasia. BMC Pediatr 12:1471-2431.

Burnett SH, Kershen EJ, Zhang J, Zeng L, Straley SC, Kaplan AM, Cohen DA. 2004. Conditional macrophage ablation in transgenic mice expressing a Fas-based suicide gene. J Leukoc Biol 75:612-623.

Cannizzaro V, Berry LJ, Zosky GR, Turner DJ, Hantos Z, Sly PD. 2009. Impact of supplemental oxygen in mechanically ventilated adult and infant mice. Respir Physiol Neurobiol 165:61-66.

Cecchini MG, Dominguez MG, Mocci S, Wetterwald A, Felix R, Fleisch H, Chisholm O, Hofstetter W, Pollard JW, Stanley ER. 1994. Role of colony stimulating factor-1 in the establishment and regulation of tissue macrophages during postnatal development of the mouse. Development 120:1357-1372.

Choi CW, Kim BI, Hong JS, Kim EK, Kim HS, Choi JH. 2009. Bronchopulmonary dysplasia in a rat model induced by intra-amniotic inflammation and postnatal hyperoxia: morphometric aspects. Pediatr Res 65:323-327.

Coalson JJ. 2003. Pathology of new bronchopulmonary dysplasia. Semin Neonatol 8:73-81.

Coalson JJ, Winter VT, Siler-Khodr T, Yoder BA. 1999. Neonatal chronic lung disease in extremely immature baboons. Am J Respir Crit Care Med 160:1333-1346.

D'Angio CT, LoMonaco MB, Chaudhry SA, Paxhia A, Ryan RM. 1999. Discordant pulmonary proinflammatory cytokine expression during acute hyperoxia in the newborn rabbit. Exp Lung Res 25:443-465.

D'Angio CT, Ryan RM. 2014. Animal models of bronchopulmonary dysplasia. The preterm and term rabbit models. Am J Physiol Lung Cell Mol Physiol 307:17.

Dai XM, Ryan GR, Hapel AJ, Dominguez MG, Russell RG, Kapp S, Sylvestre V, Stanley ER. 2002. Targeted disruption of the mouse colony-stimulating factor 1 receptor gene results in osteopetrosis, mononuclear phagocyte deficiency, increased primitive progenitor cell frequencies, and reproductive defects. Blood 99:111-120.

Daley JM, Thomay AA, Connolly MD, Reichner JS, Albina JE. 2008. Use of Ly6G-specific monoclonal antibody to deplete neutrophils in mice. J Leukoc Biol 83:64-70.

Dhaliwal K, et al. 2012. Monocytes control second-phase neutrophil emigration in established lipopolysaccharide-induced murine lung injury. Am J Respir Crit Care Med 186:514-524.

Doyle LW, Ehrenkranz RA, Halliday HL. 2014. Early (< 8 days) postnatal corticosteroids for preventing chronic lung disease in preterm infants. Cochrane Database Syst Rev 13.

Duffield JS, Forbes SJ, Constandinou CM, Clay S, Partolina M, Vuthoori S, Wu S, Lang R, Iredale JP. 2005. Selective depletion of macrophages reveals distinct, opposing roles during liver injury and repair. J Clin Invest 115:56-65.

Eriksson L, Haglund B, Odlind V, Altman M, Ewald U, Kieler H. 2014. Perinatal conditions related to growth restriction and inflammation are associated with an increased risk of bronchopulmonary dysplasia. Acta Paediatr 2:12888.

Fanaroff AA, Hack M, Walsh MC. 2003. The NICHD neonatal research network: changes in practice and outcomes during the first 15 years. Semin Perinatol 27:281-287.

Franco-Montoya ML, Bourbon JR, Durrmeyer X, Lorotte S, Jarreau PH, Delacourt C. 2009. Pulmonary effects of keratinocyte growth factor in newborn rats exposed to hyperoxia. Am J Physiol Lung Cell Mol Physiol 297:21.

Franco ML, Waszak P, Banalec G, Levame M, Lafuma C, Harf A, Delacourt C. 2002. LPS-induced lung injury in neonatal rats: changes in gelatinase activities and consequences on lung growth. Am J Physiol Lung Cell Mol Physiol 282:L491-500.

Gautier EL, et al. 2012. Gene-expression profiles and transcriptional regulatory pathways that underlie the identity and diversity of mouse tissue macrophages. Nat Immunol 13:1118-1128.

Ginhoux F, et al. 2010. Fate mapping analysis reveals that adult microglia derive from primitive macrophages. Science 330:841-845.

Gopel W, et al. 2014. Less invasive surfactant administration is associated with improved pulmonary outcomes in spontaneously breathing preterm infants. Acta Paediatr 4:12883.

Gordon S. 2003. Alternative activation of macrophages. Nat Rev Immunol 3:23-35.

Gordon S, Martinez FO. 2010. Alternative activation of macrophages: mechanism and functions. Immunity 32:593-604.

Gordon S, Taylor PR. 2005. Monocyte and macrophage heterogeneity. Nat Rev Immunol 5:953-964.

Gouon-Evans V, Rothenberg ME, Pollard JW. 2000. Postnatal mammary gland development requires macrophages and eosinophils. Development 127:2269-2282.

Groneck P, Gotze-Speer B, Oppermann M, Eiffert H, Speer CP. 1994. Association of pulmonary inflammation and increased microvascular permeability during the development of bronchopulmonary dysplasia: a sequential analysis of inflammatory mediators in respiratory fluids of high-risk preterm neonates. Pediatrics 93:712-718.

Groneck P, Speer CP. 1995. Inflammatory mediators and bronchopulmonary dysplasia. Arch Dis Child Fetal Neonatal Ed 73:F1-3.

Guilliams M, De Kleer I, Henri S, Post S, Vanhoutte L, De Prijck S, Deswarte K, Malissen B, Hammad H, Lambrecht BN. 2013. Alveolar macrophages develop from fetal monocytes that differentiate into long-lived cells in the first week of life via GM-CSF. J Exp Med 210:1977-1992.

Hanna N, Vasquez P, Pham P, Heck DE, Laskin JD, Laskin DL, Weinberger B. 2005. Mechanisms underlying reduced apoptosis in neonatal neutrophils. Pediatr Res 57:56-62.

Hayes D, Jr., Feola DJ, Murphy BS, Shook LA, Ballard HO. 2010. Pathogenesis of bronchopulmonary dysplasia. Respiration 79:425-436.

Hazinski TA, France M, Kennedy KA, Hansen TN. 1985. Cimetidine reduces hyperoxic lung injury in lambs. J Appl Physiol 67:2586-2592.

Hislop AA, Wigglesworth JS, Desai R, Aber V. 1987. The effects of preterm delivery and mechanical ventilation on human lung growth. Early Hum Dev 15:147-164.

Horbar JD, Badger GJ, Carpenter JH, Fanaroff AA, Kilpatrick S, LaCorte M, Phibbs R, Soll RF. 2002. Trends in mortality and morbidity for very low birth weight infants, 1991-1999. Pediatrics 110:143-151.

Hume DA. 2008. Differentiation and heterogeneity in the mononuclear phagocyte system. Mucosal Immunol 1:432-441.

Ingman WV, Wyckoff J, Gouon-Evans V, Condeelis J, Pollard JW. 2006. Macrophages promote collagen fibrillogenesis around terminal end buds of the developing mammary gland. Dev Dyn 235:3222-3229.

Jankov RP, Johnstone L, Luo X, Robinson BH, Tanswell AK. 2003. Macrophages as a major source of oxygen radicals in the hyperoxic newborn rat lung. Free Radic Biol Med 35:200-209.

Jenkins SJ, Ruckerl D, Cook PC, Jones LH, Finkelman FD, van Rooijen N, MacDonald AS, Allen JE. 2011. Local macrophage proliferation, rather than recruitment from the blood, is a signature of TH2 inflammation. Science 332:1284-1288.

Jobe AH, Bancalari E. Bronchopulmonary dysplasia. Am J Respir Crit Care Med. 2001 Jun;163(7):1723-9.

Jobe AH, Ikegami M. 1998. Mechanisms initiating lung injury in the preterm. Early Hum Dev 53:81-94.

Jones CA, Cayabyab RG, Kwong KY, Stotts C, Wong B, Hamdan H, Minoo P, deLemos RA. 1996. Undetectable interleukin (IL)-10 and persistent IL-8 expression early in hyaline membrane disease: a possible developmental basis for the predisposition to chronic lung inflammation in preterm newborns. Pediatr Res 39:966-975.

Jones CV, Williams TM, Walker KA, Dickinson H, Sakkal S, Rumballe BA, Little MH, Jenkin G, Ricardo SD. 2013. M2 macrophage polarisation is associated with alveolar formation during postnatal lung development. Respir Res 14:1465-9921.

Kim BI, Lee HE, Choi CW, Jo HS, Choi EH, Koh YY, Choi JH. 2004. Increase in cord blood soluble E-selectin and tracheal aspirate neutrophils at birth and the development of new bronchopulmonary dysplasia. J Perinat Med 32:282-287.

Kotecha S, Chan B, Azam N, Silverman M, Shaw RJ. 1995. Increase in interleukin-8 and soluble intercellular adhesion molecule-1 in bronchoalveolar lavage fluid from premature infants who develop chronic lung disease. Arch Dis Child Fetal Neonatal Ed 72:F90-96.

Kotecha S, Mildner RJ, Prince LR, Vyas JR, Currie AE, Lawson RA, Whyte MK. 2003. The role of neutrophil apoptosis in the resolution of acute lung injury in newborn infants. Thorax 58:961-967.

Kramer BW, Kallapur S, Newnham J, Jobe AH. 2009. Prenatal inflammation and lung development. Semin Fetal Neonatal Med 14:2-7.

Latini G, De Felice C, Giannuzzi R, Del Vecchio A. 2013. Survival rate and prevalence of bronchopulmonary dysplasia in extremely low birth weight infants. Early Hum Dev 89:70020-70023.

Lemons JA, et al. 2001. Very low birth weight outcomes of the National Institute of Child health and human development neonatal research network, January 1995 through December 1996. NICHD Neonatal Research Network. Pediatrics 107.

Li C, Fu J, Liu H, Yang H, Yao L, You K, Xue X. 2014a. Hyperoxia arrests pulmonary development in newborn rats via disruption of endothelial tight junctions and downregulation of Cx40. Mol Med Rep 10:61-67.

Li Y, Wei QF, Pan XN, Meng DH, Wei W, Wu QP. 2014b. Influencing factors for severity of bronchopulmonary dysplasia in preterm infants. Zhongguo Dang Dai Er Ke Za Zhi 16:1014-1018.

Mammel MC, Green TP, Johnson DE, Thompson TR. 1983. Controlled trial of dexamethasone therapy in infants with bronchopulmonary dysplasia. Lancet 1:1356-1358.

Margraf LR, Tomashefski JF, Jr., Bruce MC, Dahms BB. 1991. Morphometric analysis of the lung in bronchopulmonary dysplasia. Am Rev Respir Dis 143:391-400.

Martinez FO, Helming L, Gordon S. 2009. Alternative activation of macrophages: an immunologic functional perspective. Annu Rev Immunol 27:451-483.

Mascaretti RS, Mataloun MM, Dolhnikoff M, Rebello CM. 2009. Lung morphometry, collagen and elastin content: changes after hyperoxic exposure in preterm rabbits. Clinics 64:1099-1104.

Misharin AV, Morales-Nebreda L, Mutlu GM, Budinger GR, Perlman H. 2013. Flow cytometric analysis of macrophages and dendritic cell subsets in the mouse lung. Am J Respir Cell Mol Biol 49:503-510.

Munshi UK, Niu JO, Siddiq MM, Parton LA. 1997. Elevation of interleukin-8 and interleukin-6 precedes the influx of neutrophils in tracheal aspirates from preterm infants who develop bronchopulmonary dysplasia. Pediatr Pulmonol 24:331-336.

Nahrendorf M, Swirski FK, Aikawa E, Stangenberg L, Wurdinger T, Figueiredo JL, Libby P, Weissleder R, Pittet MJ. 2007. The healing myocardium sequentially mobilizes two monocyte subsets with divergent and complementary functions. J Exp Med 204:3037-3047.

Nold MF, et al. 2013. Interleukin-1 receptor antagonist prevents murine bronchopulmonary dysplasia induced by perinatal inflammation and hyperoxia. Proc Natl Acad Sci U S A 110:14384-14389.

Northway WH, Jr., Rosan RC, Porter DY. 1967. Pulmonary disease following respirator therapy of hyaline-membrane disease. Bronchopulmonary dysplasia. N Engl J Med 276:357-368.

O'Brodovich HM, Mellins RB. 1985. Bronchopulmonary dysplasia. Unresolved neonatal acute lung injury. Am Rev Respir Dis 132:694-709.

O'Reilly M, Thebaud B. 2014. Animal models of bronchopulmonary dysplasia. The term rat models. Am J Physiol Lung Cell Mol Physiol 307:10.

Ogden BE, Murphy S, Saunders GC, Johnson JD. 1983. Lung lavage of newborns with respiratory distress syndrome. Prolonged neutrophil influx is associated with bronchopulmonary dysplasia. Chest 83:31S-33S.

Ogden BE, Murphy SA, Saunders GC, Pathak D, Johnson JD. 1984. Neonatal lung neutrophils and elastase/proteinase inhibitor imbalance. Am Rev Respir Dis 130:817-821.

Paananen R, Husa AK, Vuolteenaho R, Herva R, Kaukola T, Hallman M. 2009. Blood cytokines during the perinatal period in very preterm infants: relationship of inflammatory response and bronchopulmonary dysplasia. J Pediatr 154:39-43.

Papoff P, Christensen RD, Calhoun DA, Juul SE. 2001. Granulocyte colony-stimulating factor, granulocyte macrophage colony-stimulating factor and neutrophils in the bronchoalveolar lavage fluid of premature infants with respiratory distress syndrome. Biol Neonate 80:133-141.

Pierce MR, Bancalari E. 1995. The role of inflammation in the pathogenesis of bronchopulmonary dysplasia. Pediatr Pulmonol 19:371-378.

Polglase GR, Hillman NH, Ball MK, Kramer BW, Kallapur SG, Jobe AH, Pillow JJ. 2009. Lung and systemic inflammation in preterm lambs on continuous positive airway pressure or conventional ventilation. Pediatr Res 65:67-71.

Rastogi A, Akintorin SM, Bez ML, Morales P, Pildes RS. 1996. A controlled trial of dexamethasone to prevent bronchopulmonary dysplasia in surfactant-treated infants. Pediatrics 98:204-210.

Rojas MA, et al. 2009. Very early surfactant without mandatory ventilation in premature infants treated with early continuous positive airway pressure: a randomized, controlled trial. Pediatrics 123:137-142.

Rose MJ, Stenger MR, Joshi MS, Welty SE, Bauer JA, Nelin LD. 2010. Inhaled nitric oxide decreases leukocyte trafficking in the neonatal mouse lung during exposure to >95% oxygen. Pediatr Res 67:244-249.

Rozycki HJ, Comber PG, Huff TF. 2002. Cytokines and oxygen radicals after hyperoxia in preterm and term alveolar macrophages. Am J Physiol Lung Cell Mol Physiol 282:L1222-1228.

Ryan RM, Ahmed Q, Lakshminrusimha S. 2008. Inflammatory mediators in the immunobiology of bronchopulmonary dysplasia. Clin Rev Allergy Immunol 34:174-190.

Sandri F, et al. 2004. Prophylactic nasal continuous positive airways pressure in newborns of 28-31 weeks gestation: multicentre randomised controlled clinical trial. Arch Dis Child Fetal Neonatal Ed 89:F394-398.

Schneibel KR, Fitzpatrick AM, Ping XD, Brown LA, Gauthier TW. 2013. Inflammatory mediator patterns in tracheal aspirate and their association with bronchopulmonary dysplasia in very low birth weight neonates. J Perinatol 33:383-387.

Schulz C, et al. 2012. A lineage of myeloid cells independent of Myb and hematopoietic stem cells. Science 336:86-90.

Shantsila E, Wrigley B, Tapp L, Apostolakis S, Montoro-Garcia S, Drayson MT, Lip GY. 2011. Immunophenotypic characterization of human monocyte subsets: possible implications for cardiovascular disease pathophysiology. J Thromb Haemost 9:1056-1066.

Sobonya RE, Logvinoff MM, Taussig LM, Theriault A. 1982. Morphometric analysis of the lung in prolonged bronchopulmonary dysplasia. Pediatr Res 16:969-972.

Soll RF, Morley CJ. 2001. Prophylactic versus selective use of surfactant in preventing morbidity and mortality in preterm infants. Cochrane Database Syst Rev 2.

Speer CP. 2001. New insights into the pathogenesis of pulmonary inflammation in preterm infants. Biol Neonate 79:205-209.

Speer CP. 2006. Pulmonary inflammation and bronchopulmonary dysplasia. J Perinatol 26:S63-64.

Speer CP. 2009. Chorioamnionitis, postnatal factors and proinflammatory response in the pathogenetic sequence of bronchopulmonary dysplasia. Neonatology 95:353-361.

Stefater JA, 3rd, Ren S, Lang RA, Duffield JS. 2011. Metchnikoff's policemen: macrophages in development, homeostasis and regeneration. Trends Mol Med 17:743-752.

Stein M, Keshav S, Harris N, Gordon S. 1992. Interleukin 4 potently enhances murine macrophage mannose receptor activity: a marker of alternative immunologic macrophage activation. J Exp Med 176:287-292.

Stevens TP, Harrington EW, Blennow M, Soll RF. 2007. Early surfactant administration with brief ventilation vs. selective surfactant and continued mechanical ventilation for preterm infants with or at risk for respiratory distress syndrome. Cochrane Database Syst Rev 17.

Subramaniam P, Henderson-Smart DJ, Davis PG. 2005. Prophylactic nasal continuous positive airways pressure for preventing morbidity and mortality in very preterm infants. Cochrane Database Syst Rev 20.

Sun H, et al. 2013. A critical regulatory role for macrophage migration inhibitory factor in hyperoxia-induced injury in the developing murine lung. PLoS One 8.

Sun H, et al. 2015. Prognosis of Very Preterm Infants with Severe Respiratory Distress Syndrome Receiving Mechanical Ventilation. Lung 13:13.

Syed MA, Bhandari V. 2013. Hyperoxia exacerbates postnatal inflammation-induced lung injury in neonatal BRP-39 null mutant mice promoting the M1 macrophage phenotype. Mediators Inflamm 457189:17.

Thomson MA, Yoder BA, Winter VT, Martin H, Catland D, Siler-Khodr TM, Coalson JJ. 2004. Treatment of immature baboons for 28 days with early nasal continuous positive airway pressure. Am J Respir Crit Care Med 169:1054-1062.

Tibboel J, Joza S, Reiss I, de Jongste JC, Post M. 2013. Amelioration of hyperoxia-induced lung injury using a sphingolipid-based intervention. Eur Respir J 42:776-784.

Verder H, Albertsen P, Ebbesen F, Greisen G, Robertson B, Bertelsen A, Agertoft L, Djernes B, Nathan E, Reinholdt J. 1999. Nasal continuous positive airway pressure and early surfactant therapy for respiratory distress syndrome in newborns of less than 30 weeks' gestation. Pediatrics 103.

Wagenaar GT, Sengers RM, Laghmani el H, Chen X, Lindeboom MP, Roks AJ, Folkerts G, Walther FJ. 2014. Angiotensin II type 2 receptor ligand PD123319 attenuates hyperoxia-induced lung and heart injury at a low dose in newborn rats. Am J Physiol Lung Cell Mol Physiol 307:20.

Wagenaar GT, ter Horst SA, van Gastelen MA, Leijser LM, Mauad T, van der Velden PA, de Heer E, Hiemstra PS, Poorthuis BJ, Walther FJ. 2004. Gene expression

profile and histopathology of experimental bronchopulmonary dysplasia induced by prolonged oxidative stress. Free Radic Biol Med 36:782-801.

Walsh MC, Szefler S, Davis J, Allen M, Van Marter L, Abman S, Blackmon L, Jobe A. Summary proceedings from the bronchopulmonary dysplasia group. Pediatrics. 2006 Mar;117(3 Pt 2):S52-6.

Walsh MC, et al. 2004. Impact of a physiologic definition on bronchopulmonary dysplasia rates. Pediatrics 114:1305-1311.

Wang XL, Xue XD. 2009. Anti-inflammatory effects of erythropoietin on hyperoxia-induced bronchopulmonary dysplasia in newborn rats. Zhonghua Er Ke Za Zhi 47:446-451.

Wang Y, Szretter KJ, Vermi W, Gilfillan S, Rossini C, Cella M, Barrow AD, Diamond MS, Colonna M. 2012. IL-34 is a tissue-restricted ligand of CSF1R required for the development of Langerhans cells and microglia. Nat Immunol 13:753-760.

Warburton D, et al. 2010. Lung organogenesis. Curr Top Dev Biol 90:73-158.

Weichelt U, Cay R, Schmitz T, Strauss E, Sifringer M, Buhrer C, Endesfelder S. 2013. Prevention of hyperoxia-mediated pulmonary inflammation in neonatal rats by caffeine. Eur Respir J 41:966-973.

Wiktor-Jedrzejczak W, Bartocci A, Ferrante AW, Jr., Ahmed-Ansari A, Sell KW, Pollard JW, Stanley ER. 1990. Total absence of colony-stimulating factor 1 in the macrophage-deficient osteopetrotic (op/op) mouse. Proc Natl Acad Sci U S A 87:4828-4832.

Wolkoff LI, Levine CR, Koo HC, LaGamma EF, Pollack S, Chester D, Bashore J, Davis JM. 2002. Effects of granulocyte colony-stimulating factor on hyperoxia-induced lung injury in newborn piglets. Lung 180:229-239.

Wu S, Capasso L, Lessa A, Peng J, Kasisomayajula K, Rodriguez M, Suguihara C, Bancalari E. 2008. High tidal volume ventilation activates Smad2 and upregulates expression of connective tissue growth factor in newborn rat lung. Pediatr Res 63:245-250.

Yoshida H, Hayashi S, Kunisada T, Ogawa M, Nishikawa S, Okamura H, Sudo T, Shultz LD. 1990. The murine mutation osteopetrosis is in the coding region of the macrophage colony stimulating factor gene. Nature 345:442-444.

Acknowledgements

My first gratitude goes to my supervisor, Dr E. Rory Morty, for his professional advices, help in every day work in the laboratory, teaching me how to be scientifically critical and giving me a chance to be a part of Molecular Biology and Medicine of the Lung international graduate programme.

I would like to thank Prof. Dr. Werner Seeger for his inspirational scientific discussions during lab meeting, for his kind support and for being a passion and truly dedicated scientist, inspiring for doing research.

Many thanks to all the lab members for all the moments we had together; for the unique atmosphere we had in the lab that helped me to work with pleasure. Special thank to Gero Niess, Simone Becker and Lukasz Wujak who I started my PhD with and who made it really easy for me.

I really don't know if I would make it without my friend and co-worker Akis Sakkas. He became a true friend for me, supported me a lot in every-day life in the institute and will stay my dear friend after we finish PhD and move to different countries.

My special thank you to my husband Anuar Kalymbetov, who always believed in me, supported me in difficult times and was proud of me when I gained something in life. And who inspired me to move to Europe to perform PhD and made this decision and life far away from home easy for me. .

I would also like to thank my old friend Alena Moiseenko, who I know since primary school and who I went to the same university with. Having her here thousands kilometres away from home was truly great and helped me to manage through all the difficult times during my PhD.

My last but not least gratitude goes to my family: my parents, my sister and her son, my aunt and uncle and my grandparents, who are my support in life and there are no words to describe what they mean to me and how much they support me in important decisions I make. Without them I would not be at the point I am now.

Declaration

Hiermit erkläre ich, dass ich die vorliegende Arbeit selbständig und ohne unzulässige Hilfe oder Benutzung anderer als der angegebenen Hilfsmittel angefertigt habe. Alle Textstellen, die wörtlich oder sinngemäß aus veröffentlichten oder nichtveröffentlichten Schriften entnommen sind, und alle Angaben, die auf mündlichen Auskünften beruhen, sind als solche kenntlich gemacht. Bei den von mir durchgeführten und in der Dissertation erwähnten Untersuchungen habe ich die Grundsätze guter wissenschaftlicher Praxis, wie sie in der „Satzung der Justus-Liebig-Universität Gießen zur Sicherung guter wissenschaftlicher Praxis“ niedergelegt sind, eingehalten sowie ethische, datenschutzrechtliche und tierschutzrechtliche Grundsätze befolgt. Ich versichere, dass Dritte von mir weder unmittelbar noch mittelbar geldwerte Leistungen für Arbeiten erhalten haben, die im Zusammenhang mit dem Inhalt der vorgelegten Dissertation stehen, oder habe diese nachstehend spezifiziert. Die vorgelegte Arbeit wurde weder im Inland noch im Ausland in gleicher oder ähnlicher Form einer anderen Prüfungsbehörde zum Zweck einer Promotion oder eines anderen Prüfungsverfahrens vorgelegt. Alles aus anderen Quellen und von anderen Personen übernommene Material, das in der Arbeit verwendet wurde oder auf das direkt Bezug genommen wird, wurde als solches kenntlich gemacht. Insbesondere wurden alle Personen genannt, die direkt und indirekt an der Entstehung der vorliegenden Arbeit beteiligt waren. Mit der Überprüfung meiner Arbeit durch eine Plagiatserkennungssoftware bzw. ein internetbasiertes Softwareprogramm erkläre ich mich einverstanden.

_____ _____

Ort, Datum Unterschrift